Petrogenesis of PGE mineralised intrusions in the floor of the northern Bushveld Complex

Wolfgang D Maier, School of Earth and Environmental Sciences, Cardiff University, UK, Email: maierw@cardiff.ac.uk

Albie Brits*, Ivanplats Ltd, Mokopane, South Africa, Email: abrits@criticalminerals.com

Danie Grobler*, Ivanplats Ltd, Mokopane, South Africa, Email: dgrobler@criticalminerals.com

*Present address : Stillwater Critical Minerals, Vancouver, Canada

Abstract

The floor rocks of the northern lobe of the Bushveld Complex host several sill-like mafic-ultramafic bodies. In the present paper we evaluate whole rock data generated by exploration companies for sills on the farms Townlands, Amatava, Uitloop, Turfspruit and Rietfontein, located to the north of Mokopane, in order to constrain the origin of the sills and their mineralisation. Key observations include: (i) The sills have geochemical affinities to the Lower Zone (LZ) or Lower Critical Zone (LCZ). (ii) Most sills are enriched in sulphides and platinum-group elements (PGE) relative to most other LZ and LCZ cumulates. (iii) Most PGE mineralised intrusives have been emplaced into the carbonaceous-pelitic Duitschland Formation. (iv) The sills are spatially associated with the Mokopane gravity anomaly, possibly representing a major feeder zone to the Bushveld Complex. (v) The sills show evidence for assimilation of the sedimentary host rocks in the form of locally elevated $\delta^{34}S$, incompatible trace element contents and the presence of carbonaceous and pelitic country rock xenoliths. (vi) There is no correlation between PGE abundance and indicators of crustal contamination. Based on these data we propose that in the vicinity of the putative Mokopane feeder zone relatively fertile, unevolved magmas ascended through the crust initially as dykes. When intersecting the relatively fissile Duitschland Formation the mode of magma emplacement changed to one of sills. This facilitated contamination with sulphide- and graphite-rich carbonate and shale, triggering sulphide melt saturation. The sulphides were locally entrained and upgraded within the sills before precipitating, likely within flow dynamic traps.

Introduction

The Bushveld Complex is the most valuable ore belt on Earth, hosting the bulk of the world's PGE, V and Cr resources, as well as significant Ni and Cu. The northern lobe of the complex is particularly important as it has become the focus of PGE exploration culminating in the recent discovery of the Flatreef and Waterberg reef-style and contact-style PGE deposits (see reviews in Kinnaird and McDonald, 2018, and Maier et al., 2021a). In contrast, the key exploration targets for magmatic Ni-Cu-(PGE) deposits, in the Bushveld and globally, are relatively small sill-, dyke- and funnel-shaped intrusives that may represent feeder conduits (Barnes et al., 2016). In the Bushveld, the key example is Uitkomst, a sulphide- and chromite-rich satellite intrusion discovered almost a century ago (Wagner, 1929) and mined for Ni-Cu-PGE sulphides and chromite since 1997. However, no other examples of economically viable sills have been found associated with the Bushveld Complex so far. Here we present data on mineralised footwall intrusives in the northern lobe of the Bushveld Complex. Our main aim is to constrain the stratigraphic setting and geochemical lineage of the intrusives and the origin of their mineralisation. We further discuss general implications for the origin of, and exploration for, the Bushveld PGE mineralisation.

Geological setting

In the classical localities of the western and eastern lobes of the Bushveld Complex (WBC and EBC, respectively), the intrusion consists of a 6-10 km pile of ultramafic and mafic cumulates, emplaced mostly into the predominantly pelitic Timeball Hill Formation of the Transvaal Supergroup. The cumulates show a broadly progressive trend of differentiation with height (albeit interrupted by numerous reversals), from ultramafic rocks in the Lower Zone (LZ) and Lower Critical Zone (LCZ), to interlayered ultramafic and mafic rocks in the Upper Critical Zone

(UCZ), predominantly gabbronoritic rocks in the Main Zone (MZ), and interlayered gabbroic-dioritic-anorthositic rocks with numerous magnetite layers in the Upper Zone (UZ)(Maier et al., 2013).

In a broad sense this stratigraphy can also be applied to the northern lobe, although there are certain differences. Firstly, the northern lobe magma was emplaced discordantly into a range of footwall lithologies (Kinnaird and McDonald, 2018; Maier et al., 2021a, and references therein): To the south of Mokopane, the country rocks comprise quartzite and shale of the Timeball Hill Formation, Transvaal Supergroup. Further to the north, progressively lower units of the Transvaal Supergoup have been intruded, namely shale and dolomite of the Duitschland Formation from Mokopane to the farm Turfspruit, ironstone of the Penge Formation on the farm Tweefontein, and dolomite of the Malmani Subgroup on the farm Sandsloot. In the remainder of the northern lobe, the footwall to the Bushveld Complex consists of Archaean granite-gneiss basement. Amongst the footwall lithologies, shale and dolomite appear to be relatively more readily assimilated, resulting in numerous xenoliths of variable size, and interfingering of the floor rocks with the lower and central portions of the Bushveld Complex (including the LZ, CZ and MZ) expressed by numerous sill-like intrusives within the sediments (Wagner, 1929; Manyeruke et al., 2005; Kinnaird, 2005; Grobler et al., 2019). As a result, the contact between the Bushveld Complex *sensu strictu* and the floor rocks becomes difficult to delineate. Secondly, there are certain stratigraphic differences: (i) The LZ of the northern lobe appears to form distinct sill-like bodies of up to 1700 m combined thickness separated from the remainder of the complex by a screen of sediments (Hulbert, 1983; Maier et al., 2008; Yudovskaya et al., 2013). (ii) The LCZ appears to be missing. (iii) The UCZ and UZ have highly variable thickness showing a general trend of thinning towards the North, with both locally missing (e.g., the CZ at Nonnenwerth and the Waterberg deposit, and the MZ to the south of the farm Altona).

From an economic point of view it is particularly noteworthy that in the northern Bushveld lobe, the entire UCZ is significantly more sulphide- and PGE-mineralised than in the western and eastern lobes which led to the coining of the term Platreef (Van der Merwe, 1976). More recently, the name “Flatreef” has been introduced for the down-dip extensions of the Platreef on the farm Turfspruit, in view of the flattening of the dip at this locality (Grobler et al., 2019).

In the present study we describe sill-like intrusives of variable thickness (~80 m to > 1000 m) on the farms Townlands, Amatava, Uitloop, Turfspruit and Rietfontein, to the north of Mokopane (Figure 1). The intrusives are predominantly of ultramafic composition, but they may also contain noritic or, locally, gabbronoritic intervals. The area is of particular exploration interest because it is located proximal to the largest gravity anomaly in the Bushveld, potentially representing a major feeder zone (van der Merwe, 1978; Finn et al., 2015; Cole et al., 2021). The studied intrusives occur at various stratigraphic levels, (i) in the immediate footwall of the UCZ/Platreef (on Townlands), (ii) within sedimentary rocks of the Duitschland Formation several 100 m below the Platreef (on Uitloop and Amatava), and (iii) within the Archaean basement granite (on Uitloop and Rietfontein).

Analytical methods

Samples from Uitloop, Amatava, Rietfontein and Townlands were analysed by a range of commercial laboratories, including Ultra Trace, Setpoint, and Lakefield. The analytical methods used included XRF (for major and trace elements including base metals), fire assay with ICP-OES finish (for Pt, Pd and Au), Leco titration (for S), and microscope study of polished and covered thin sections. The detection limit for the PGE and Au varied between laboratories and inevitably

this introduces some bias in some of our data plots. Set Point laboratories who analysed Rietfontein drill cores **RF4 and 2** as well as the Amatava and Uitloop drill cores quote a detection limit of 10 ppb for Au, Pt, Pd and Rh, 10 ppm for Cu, Ni, Co, and 0.01 wt.% for S. Ultra Trace laboratories which analysed Rietfontein drill cores **RF6, 5 and 1** quote a detection limit of 1 ppb for PGE and Au, 5 ppm for Ni, Cu, Co, 10 ppm for Cr, and 0.01 wt.% for S. Lakefield laboratories were involved in Ni-Cu-Co assaying and quote a detection limit of 20 ppm for these elements. All laboratories applied rigorous quality control, including regular analysis of a range of standards and duplicates together with the samples and extensive statistical evaluation of accuracy and precision, reported in unpublished company reports. In order to obtain data on the full spectrum of PGE, we further analysed six samples from drill core Uit 01-01 using Instrumental Neutron Activation Analysis (INAA) at the University of Quebec at Chicoutimi (Table 1).

The lithophile element data for samples from the Uitloop I body are presented in Table 2. The samples were analysed applying the standard method used in the XRF laboratory of the University of Pretoria, as adapted from Bennett and Oliver (2002). Major elements were determined on fused beads, and trace elements were determined on pressed powder briquettes prepared following the method of Watson (1996). Precision and accuracy were monitored by running a range of standards with each suite of unknowns, suggesting that the analytical error for major and minor elements is generally below 5 %, whereas for trace elements it may reach ~10%. CIPW norms of the samples were calculated using the program of Hollocher (2004).

Sulphur isotopes were determined for a range of samples from the Uitloop II body at Indiana University, USA (Table 3). Sulphide powders and small amount of V_2O_5 were loaded into tin capsules and analysed using Elemental Analyzer-Continuous Flow Isotope Ratio Mass

Spectrometry on a Finnigan MAT252 isotope ratio mass spectrometer. Analytical precision is better than +-0.05‰. Sample reproducibility is +- 0.1‰.

Description of samples and drill cores

Sills in the immediate footwall of the Platreef

A number of mafic-ultramafic bodies occur in the sedimentary footwall of the Platreef unit on the farm Townlands, within the lower Timeball Hill Formation of the Pretoria Group, Transvaal Supergroup. Bore holes TL 01-01 and 01-02, located ~1.2 km to the NE of the collar of bore hole TL 01-03 (which intersects lower Platreef and was studied by Manyeruke et al., 2005) intersect thick sills of interlayered harzburgite, dunite and pyroxenite interpreted to represent the Lower Zone (LZ) by Falconbridge Ventures of Africa. This interpretation is consistent with Yudovskaya et al. (2013) who described putative LZ below the Platreef at several locations in the northern Bushveld lobe.

Bore hole TL 01-2 (dip ~50°, azimuth ~47°) has been collared just 200 m to the NE of the mapped basal contact of the Platreef unit (Figure 1). The borehole intersects shale until ~ 85 m and, below that, the strongly fractured contact to fine-grained orthopyroxenite which grades (after ~ 5 m) into medium-grained pyroxenite and then interlayered harzburgite and pyroxenite (with gradational contacts between lithologies), until the end of the hole at 185 m. Narrow gabbroic layers and sedimentary interlayers or xenoliths occur in the basal 13 m of the drill core. Traces of pyrrhotite and pyrite occur throughout. The orientation and dip of igneous layering are unknown.

Borehole Tl 01-1 (dip ~51°, azimuth ~55°) has been collared 300 m to the NE of TL 01-2. The hole intersected ~6 m of overburden and then 515 m of interlayered medium-grained harzburgite and orthopyroxenite containing large orthopyroxene oikocrysts. The rocks are locally pervasively serpentinised and cut by several granitic dykes. The orientation and dip of layering are unknown.

Unfortunately, the composition of the putative LZ sills intersected by the TL 01-01 and -02 boreholes remains poorly known since no assays were produced, likely because the rocks contain only very sparse sulphides.

Sills in the sedimentary floor rocks of the Lower Zone on the farms Uitloop and Amatava

Boreholes drilled by Falconbridge Ventures of Africa on the farms Uitloop 3KS and Amatava 41KS along a NW-SE striking drill line, ~ 800 m to the NE of the putative LZ bore holes on Townlands discussed above (Figure 1), intersected a sill of pyroxenite with local development of harzburgite and norite. The sill was emplaced into shales and carbonates of the Duitschland Formation, a few meters to 10s of meters above the contact between the Duitschland Formation and the Penge iron formation. The sills likely form a laterally continuous body, striking ~ 140° and dipping 20-30° to the SW. Note that the Penge iron formation has a steep near surface dip (>60°) probably due to pre-existing folding of the Transvaal strata close to the Rooisloot – Nkwe fault intersection (Figure 2a). Open folding has also been observed on Macalacaskop (unpublished data of authors). Figure 2 also shows the expected transgressive relationship with the mafic/ultramafic units/sills.

177 The thickness of this body is highly variable (Figure 2b); In the NW (drill core Uit 01-05)
178 and SE (drill cores Uit 01-01 and Am 99-1 and 99-2) the sill is ~100 m thick and entirely hosted
179 within the sediments of the Duitschland Formation, but in the centre of the study area the sill
180 has a thickness of > 200 m and is sub-cropping. It is proposed that the sill forms part of the lower
181 portion of the ~600 m thick Uitloop II ultramafic body described in van der Merwe (1978). In the
182 NW and SE (near the Uitloop-Amatava farm boundary), where the bore hole collars are within
183 sediments, the sill may form a footwall apophysis of the Uitloop II body.

184

185 *Farm Uitloop 3KS*

186 Drill core Uit 01-01 (Dip 50°, Azimuth 58°) intersected ~100 m of sulphide mineralised, medium-
187 grained melanorite and pyroxenite, locally containing “sugary” textured, finely layered chromite.
188 The intrusives were emplaced into carbonate and diamictite of the Duitschland Formation, some
189 30 m above the Penge iron formation (Figure 2a). Ninety-eight samples were assayed for Fe, Ni,
190 Cu, Co, Au, S, Pt and Pd. In addition, major elements were determined in seven samples using
191 XRF. The analysed samples contain 13-28 wt. % MgO and 0.4-1.06 wt.% Cr_2O_3. Their CIPW norms
192 suggest that the intrusion consists mostly of mela(gabbro)norite, with minor olivine (8-10 modal
193 %) in the upper portion. Values of FeO contents in the rocks are mostly 8-10 wt.%, suggesting ~
194 40-70 % modal orthopyroxene. Locally higher Fe contents are due to the presence of up to 6
195 wt.% sulphides, notably in the upper portion of the intrusion, and in its lowermost ~6 m which is
196 a hybrid rock interpreted to be diamictite and consisting of grey-green, fine-grained mafic
197 material as well as light-grey, fine-grained sedimentary material. In addition, there are dirty-
198 white, fine-grained siliceous BIF fragments. The Mg# of the silicate fraction in the sill is up to

199 0.86, in the range of typical LZ or LCZ. PGE and Ni contents broadly correlate with sulphide
200 content, albeit showing some scatter (Figure 3).

201 The elevated Fe contents of the lower 10-15m of the sill (Figure 4) coincide with relatively
202 low MgO and elevated K_2O and normative biotite, suggesting a relatively evolved, possibly
203 strongly contaminated basal unit. The average K_2O content of the seven samples for which
204 comprehensive whole rock data are available is 0.46 wt.%, broadly analogous to the Platreef
205 (Ihlenfeld and Keays, 2011), but markedly higher than in the UCZ of the WBC (Maier et al., 2013).

206 The entire sill is PGE-mineralised, with grades ranging from ~80 ppb Pt+Pd+Au to peak
207 values of 3.4 ppm Pt+Pd+Au, the latter in the basal hybrid rock (Figure 4). There is not a single
208 sample that has PGE contents in the range expected from a cumulate that crystallised from
209 sulphur-undersaturated B1 magma (i.e., < 20-30 ppb Pt+Pd). Average PGE contents over 100 m
210 are 0.293 ppm Pt and 0.184 ppm Pd (0.477 ppm Pt+Pd). Palladium/iridium ratios are relatively
211 high, between ~ 100 and > 1000, showing a progressive increase with depth (Figure 4, Table 1).
212 Values of $\delta^{34}S$ range from +8 to +12, indicating the presence of crustal sulphides (Table 2).

213 Drill core Uit 01-03 (Dip 52°, Azimuth 50°) intersected crudely layered, medium- to
214 coarse-grained harzburgite and olivine-orthopyroxenite, interlayered at its base with
215 sedimentary rocks (ESM 1). Whole rock data are available for seven samples, indicating MgO
216 contents of 27-42 wt.%. Only one sample has significant normative clinopyroxene (27 modal %).
217 The Mg# of the silicate fraction is 0.83-0.89, higher than in typical UCZ rocks from the WBC or
218 the Platreef, and consistent with a LZ or LCZ lineage. K_2O is much lower (0.09 wt.%) than in drill
219 core Uit 01-01. PGE contents are also much lower (maximum of 0.15 ppm), although sulphur
220 contents can be in the range of drill core Uit 01-01 (i.e. up to ~3 wt.% S) with up to 2 modal %
221 interstitial sulphides reported from many intervals. Values of $\delta^{34}S$ range from +9 to +15, again

222 indicating the presence of crustal sulphides (Table 2). The floor rocks consist of ~7 m of Penge
223 iron formation which in turn is underlain by ~35 m of banded limestone and mudstone assigned
224 to the Malmani Subgroup.

225 Drill core Uit 01-02 (Dip 88°, azimuth 70°) intersected 250 m of dolomite, banded oxide-
226 rich mudstone and graphitic shale, assigned to the Malmani Subgroup. No intrusives were
227 intersected. Four samples were analysed for S and PGE. Sulphur peaked at 2.4 wt. %, but none of
228 the analysed samples contained PGE above the detection limit (10 ppb for Pt and Pd each).

229 Drill core Uit 01-04 (Dip 53°, Azimuth 51°) intersected poikilitic harzburgite (until ~63 m)
230 and several pyroxenite sills within limestone of the Duitschland Formation. Weakly disseminated
231 pyrite (< 0.5 modal %) is not uncommon. No assays are available.

232 Drill core Uit 01-05 (Dip 50°, Azimuth 62°) intersected ~100 m of norite (ESM 2). Whole
233 rock data for four samples show 16-19 wt.% MgO, and CIPW norms indicate 44-53 %
234 orthopyroxene, 27-31 % plagioclase and 3-7 % clinopyroxene. The Mg# of the silicate fraction
235 reaches 0.86. The sill becomes slightly less evolved with depth, in contrast to, e.g., drill core Uit
236 01-01. At the top of the sill (72.68-73.44 m) is a breccia zone of mixed greenish-grey carbonate
237 and fine-grained, light-grey mafic intrusive, the latter interpreted as a chilled margin. This is
238 underlain by massive melanorite (~50 normative % orthopyroxene, 35 % plagioclase, 5 %
239 clinopyroxene and 5 % quartz) until 143.1 m, containing carbonate xenoliths near the top. From
240 143.1 to 147.7 m there are several dolomite xenoliths. The remainder of the sill (to 178.47 m)
241 consists of massive melanorite. No assay data are available for that portion. The upper 60 m of
242 the sill contain weakly disseminated sulphides and PGE contents mostly below the detection
243 limit of 10 ppb for Pt and Pd. Below a depth of 130 m, sulphide contents increase to ~2 modal %

244 (one sample has 1.7 wt.% S), Cu increases from 600 ppm to 2100 ppm, Ni from ~800-900 ppm to
245 > 3000 ppm, and PGE+Au contents increase to > 1 ppm (peaking at 2.8 ppm).

246

247 *4.3.2 Farm Amatava 41KS*

248 Bore hole Am 99-2 (Dip 50°, Azimuth 50°) intersects 42 m of saprolite and then melanorite with a
249 few mela olivine-norite or harzburgite layers as well as sedimentary xenoliths until 110.62 m
250 (Figure 5). The lower portion of the intersection (at 93.3 m, 105.87-107.25 m, and 110.62- 122
251 m) contains several layers characterised by a fine-grained, partly altered rock consisting of
252 quartz, amphibole, orthopyroxene and clinopyroxene, with fragments of chert and carbonate
253 and up to 5% blebby, disseminated and stringer-type pyrite / pyrrhotite mineralisation. The rocks
254 have been termed “tactites” by Falconbridge geologists and were interpreted as altered
255 hornfels. However, the tactites contain between 4.7 and 9.6 wt.% MgO and thus could
256 alternatively represent chilled and contaminated products of the intruding magma. In the
257 following they are thus referred to as fine-grained contact rocks. They are underlain by
258 diamictite, consisting of a matrix-supported shale/mudstone breccia, containing quartz, chert
259 and calcite clasts up to 4 cm in length, with pyrrhotite and pyrite veins and disseminations. From
260 156.95 m to 158.63 m there is fine-grained black shale which is underlain by Penge iron
261 formation.

262 CIPW norms indicate that the upper melanorite contains 60-70 % orthopyroxene, 20%
263 plagioclase, and minor clinopyroxene and olivine. The most mafic portions of the olivine
264 melanorite have up to 45% olivine, 35% orthopyroxene and 15% plagioclase, with estimated Mg#
265 in the silicate portion of the rock at ~0.87. The quartz-norite has 50-60 % orthopyroxene, 5-10 %
266 clinopyroxene, 20 % plagioclase and 5-10 % quartz.

Apart from the interval between ~70 m to 80 m the drill core contains visible sulphides (mostly < 1 wt%, but locally up to several percent). As in most of the intersections from the farm Uitloop, PGE contents are elevated throughout most of the analysed portion of the drill core, ranging between ~0.1 – 1.3 ppm. However, most of the fine-grained contact rocks have PGE below the detection limit, except for a few samples that contain several % sulphides, up to 400 ppm Cu and 300 ppb Pt+Pd. The diamictites contain up to 200 ppm Cu but are barren of PGE. One sample has been analysed for S isotopes, showing a value of $\delta^{34}S$ of approximately +6.5 (Table 2).

Drill core Am 99-1 (Dip 50°, Azimuth 50°) intersects a ~100 m sill of melanorite with mela olivine norite (or harzburgite) layers, emplaced into limestone and shale of the Duitschland Formation. The sill is outcropping / sub-cropping as indicated by a pronounced Ni-in-soil anomaly (ESM3). The stratigraphy is broadly similar to that in Am 99-2. At the top is fine-grained contact rock (55.62-65.89 m and 69.55-70.38 m) having relatively high MgO contents of 9-12.45 wt.%. This is underlain by quartz-bearing melanorite (until ~110 m) containing ~60 % normative orthopyroxene, 20 % plagioclase, 5-10 % clinopyroxene and up to 5 % quartz (Figure 6). The next 10 m consist of olivine melanorite, with ~50 % normative olivine, 10-30 % orthopyroxene, 10-20 % plagioclase and minor clinopyroxene (Mg# in the silicate fraction is as high as 0.9). Most of the remainder of the sill consists of melanorite, with 50-70 % normative orthopyroxene, 20 % plagioclase, up to 10 % clinopyroxene and minor quartz. Dolerite is intersected at 127.38-134.54 m. In the basal few meters, plagioclase reaches 30 % of the norm, and there are fine-grained intrusives and contact rocks (6-9.5 wt.% MgO, up to 2 wt.% sulphide, PGE below detection limit).

Analogous to some other drill cores intersecting the Uitloop II body, including Uit 01-01 and AM 99-2, the entire AM 99-1 drill core contains more PGE than the 10-30 ppb Pt+Pd that

290 could be assigned to a (trapped) liquid component. However, in the present drill core the PGE
291 tend to be concentrated in the lower portion of the intrusion, and peak values are ~0.7 ppm, i.e.,
292 lower than at Uit 01-01. Sulphide contents reach ~ 2.5 wt.% (~1 wt.% S) and show a good
293 positive correlation with PGE contents. Cu/Pd is mostly 1000-3000, indicating a fertile parent
294 magma. The bottom and top portions of the sill have higher Cu/Pd (Figure 6) consistent with
295 these rocks containing a trapped melt component. In general, Pd/Ir is much higher (~80-240)
296 than in the Platreef, consistent with our data from Uit 01-01, whereas Cu/Ni is lower (0.2 to 0.3).
297 Pt/Pd is 0.5-1, in the range of the Platreef. The interval with elevated PGE has the lowest Pt/Pd
298 ratios (avg. 0.51). There is no enrichment in K_2O or Zr within the PGE enriched horizon, providing
299 little indication of a role for contamination in triggering the mineralisation. Similarly, CaO/Al_2O_3 =
300 0.6-1, in the range of typical CZ rocks. However, one sample analysed for S isotopes yielded a
301 value of $\delta^{34}S$ of +12, indicating the presence of crustal sulphides (Table 2).

302 The base of the sill is characterised by a decrease in MgO, Mg# and Cr, and an increase in
303 K_2O and Zr (Figure 6) which could suggest interaction with crustal material. The floor rocks
304 consist of diamictite (163.8 - 180.12 m) and, below that, Penge iron formation.

305

306 Sills in the Archaean basement

307 *Farm Uitloop 3KS*

308 An ultramafic sheet-like body measuring approximately 4x3 km in outcrop occurs within
309 Archaean granite gneiss of the eastern portion of the farm Uitloop 3KS and the western part of
310 the farm Bloemhof 4KS. The body was named Uitloop I by van der Merwe (1978) from whom
311 much of the following description is taken, in addition to field observations made by the senior
312 author. Note that the numbering of the body should not be confused with the drill core numbers

313 from the Uitloop II body (Uit 01-01 to 01-05). The Uitloop I body shows faint layering, striking ~
314 130° with a dip of 20-30° to the SW, and an estimated thickness of 2100 m. It forms a prominent
315 hill, named Mohale Sedikwe, that is surrounded by scree slope. The body displays a well-
316 developed joint system striking W to WNW. Its northwestern boundary strikes sub-parallel to the
317 Mahopani fault, and further postulated faults trending NE suggest that the entire body could be
318 fault-bounded. Van der Merwe (1978) described a fine-grained olivine-bearing chilled phase at
319 the base, overlain by 300 m of medium-grained orthopyroxenite adcumulate showing highly
320 equilibrated microtextures and, locally, chromite lenses. The orthopyroxenite is overlain by a ~30
321 m noritic layer containing abundant argillaceous xenoliths and then >1100 m of texturally highly
322 equilibrated medium-grained orthopyroxenite adcumulate, 400 m of serpentinite and 300 m of
323 olivine orthopyroxenite. Boulders of fine-grained norite along the western margin could suggest
324 the presence of an upper chilled margin phase.

325 Twenty-two samples of orthopyroxenite were collected during a field visit in 2001 by the
326 first author and S. de Waal, traversing the body roughly from stratigraphically relatively low
327 horizons in the NE to stratigraphically higher horizons in the SW (Table 2). The rocks are
328 compositionally remarkably homogeneous, with more than 90 normative % orthopyroxene, the
329 remainder being largely made up of interstitial plagioclase, minor poikilitic clinopyroxene and
330 traces of chromite. This compositional homogeneity constitutes the main difference to most
331 ultramafic rocks from the LZ and CZ elsewhere in the Bushveld (Figure 7a,b). Another notable
332 feature is the relatively high MgO content of the Uitloop I pyroxenites, a feature that is
333 characteristic of many northern lobe LZ rocks, whereas LZ rocks of the western lobe tend to have
334 lower MgO (Yudovskaya et al. 2013).

335 The body has low S (mostly < 100 ppm) and Cu contents (mostly < 10 ppm)(Table 2). The
336 stratigraphically lowermost rocks show a subtle enrichment in Cu, S, Zr, Sr, Rb, Cl. This could
337 reflect minor contamination with the granite gneiss basement or the presence of an enhanced
338 proportion of trapped melt. Mg# in the silicate fraction of the rocks is up to 0.91, increasing
339 slightly towards the south, i.e., with increasing stratigraphic height. Incompatible trace element
340 contents suggest a liquid fraction of ~10-20 %, assuming a B1-type parent magma (Barnes et al.,
341 2010).

342

343 *Rietfontein*

344 Rietfontein is a sheet-like body with a length of ~3 km (striking NW), a width of ~500 m and a
345 stratigraphic thickness of ~ 265 m (van der Merwe 1978) (Figure 1). It consists of several sheets
346 (ESM4), dipping at ~40° to the west, and emplaced near the contact between the Malmani
347 dolomite and Archaean basement, on the farms Rietfontein and Holmesleigh. The roof dolomite
348 has been thermally metamorphosed over several meters. Lithological and petrographic
349 descriptions by van der Merwe (1978) indicate that the intrusion consists largely of
350 orthopyroxenite commonly forming adcumulates, with layers of harzburgite, olivine pyroxenite
351 and norite. Olivine heteradcumulates tend to be strongly serpentinised. In addition to medium-
352 grained olivine, the latter rocks contain poikilitic orthopyroxene and clinopyroxene, locally
353 altered to hornblende. Olivine-orthopyroxenites are less altered. They have variable grain size
354 (0.5-3.5 mm) and show elongated or equigranular grain morphologies with equilibrated
355 microtextures expressed by rounded grain boundaries and 120° triple junctions. Chromite and
356 intercumulus plagioclase are minor components. Van der Merwe (1978) analysed one sample of
357 olivine heteradcumulate and obtained Fo content of olivine of 87.

A drilling campaign by Platreef Resources in 2002 comprised six bore holes, drilled sub-vertically (RF5 and 6) or at ~50° dip (RF1-4). The holes intersected several intrusive sheets with a maximum apparent thickness of ~600 m (RF5) (ESM 5). Rock types included orthopyroxenite, olivine pyroxenite, harzburgite and norite. Contacts between layers can be sharp or gradational (Figure 8). The assay data of Platreef Resources indicate that most of the rocks are pyroxenites and olivine-pyroxenites with 500-1000 ppm Ni and 2000-5000 ppm Cr. However, there are also numerous samples with higher Ni (up to ~2500 ppm) and Cr (up to ~ 15000 ppm), representing harzburgites that may contain appreciable chromite (Figure 9a). Drill core RF1 intersected a predominantly noritic portion of the intrusion, with 100-400 ppm Ni (Cr contents are not available). Sample 82 in van der Merwe (1978) has 6.56 wt. % MgO and 23.5 wt.% Al_2O_3 and may thus be derived from this portion of the intrusion. It has a CIPW norm of 82 % plagioclase, 11 % orthopyroxene, and 6 % olivine. The modelled Fo content is 69, Mg# in the silicate fraction is 0.76 and An content of plagioclase is 83.6, i.e., the rock appears to be a moderately evolved olivine leuconorite.

All intersected rock types are PGE mineralised, but orthopyroxenites and, to a lesser degree, norites appear to be particularly prospective. Peak Pt+Pd values are 0.8 ppm (Pt/Pd 0.5-2), but the bulk of the samples have < 0.4 ppm (Figure 9b, c). Samples with < 30 ppb PGE are rare, analogous to the Uitloop II body. The PGE contents are mostly not correlated with S or Cu contents (Figure 9d), although some of the most PGE rich samples have several 100 ppm Cu (max 3000 ppm).

Plots vs height (e.g., drill core RF6, Figure 10) show that the intrusion contains thick intervals of compositionally relatively homogeneous orthopyroxenites (3000-5000 ppm Cr, 800 ppm Ni) as well as intervals of interlayered olivine-pyroxenite, pyroxenite and harzburgite (>1500

ppm Ni). At the top and base of the intrusion there occur some feldspathic intrusives that are possibly of gabbronoritic composition. Note that PGE are relatively enriched in the homogeneous, S poor pyroxenite. In contrast, the relatively more layered intervals are more S rich and typically PGE poor.

The assay data indicate relatively sharp boundaries between the central, sulphur poor - PGE rich pyroxenite and the S-, Ni-, Cr-rich and PGE poor olivine-rich lithologies. The basal and top sequences appear to be of broadly similar composition, possibly suggesting that the PGE-rich pyroxenite in the centre intruded as a sill.

Discussion

Location and geological setting of floor sills

The studied sills are located 7-15 km to the north of Mokopane, forming a N-S trending belt in the footwall of the northern lobe of the Bushveld Complex. Three further ultramafic bodies not studied here (Zwartfontein and Bultongfontein I + II) occur a further 6-7 km northwards. The Bultongfontein bodies intruded into Archaean basement granite. They are up to ~1 km thick and consist predominantly of orthopyroxenite. The body on the farm Zwartfontein is the northernmost of the known floor intrusives. It is ~900 m thick, intruded into basement granite, and consists largely of orthopyroxenite with several chromitite layers as well as some olivine-orthopyroxene cumulates. The Bultongfontein and Zwartfontein bodies have been assigned to the LZ by van der Merwe (1978). To our knowledge, no information exists on PGE contents in the intrusives.

The sills studied in the present work have highly variable thicknesses, between 90 m (Uitloop II body) to 2100 m (Uitloop I body). Their exposed strike length is up to ~3 km. The dip of the layering is broadly similar to that of the main Bushveld Complex in the northern lobe, at 20-40° to the west, whereas the sedimentary host rocks dip at ~ 55°- 65° to the west. The sills are mostly hosted within the basal portion of the Transvaal Supergroup, i.e., the Duitschland Formation (Uitloop II and Amatava) and the Malmani Subgroup (Rietfontein). Uitloop I (as well as Bultongfontein and Zwartfontein) are hosted within the uppermost portion of the basement granite, near the contact with the Transvaal Supergroup.

Magmatic lineage and stratigraphic correlation of floor sills

(i) General

All economic PGE deposits of the Bushveld Complex, including the Platreef/Flatreef, UG2 chromitite and Merensky Reef occur in the UCZ. Establishing whether the floor sills are of UCZ, LCZ or LZ compositional lineage is thus of potential exploration interest. The different zones of the Bushveld Complex are characterised by contrasting lithologies and compositions, although there is some overlap. The LZ consists almost entirely of ultramafic rocks, including harzburgite and dunite (making up ~60% of the LZ at Union Section, Teigler and Eales 1996), and orthopyroxenite (40% of LZ at Union Section). The LCZ is dominantly orthopyroxenitic, containing ~10 chromitite seams. Both the LZ and the bulk of the LCZ typically have Mg# of orthopyroxene in excess of 0.85 (Teigler and Eales, 1996), and low contents of PGE (<100 ppb) and sulphur (<200 ppm) (Maier et al., 2013), with the exception of the LCZ chromitites that may contain up to 3 ppm PGE (Naldrett et al., 2009; Scoon and Teigler, 1994) and certain sulphide-enriched intervals of the northern lobe LZ that may have several 100 ppb combined Pt+Pd (Hulbert & von

425 Gruenewaldt, 1982; Tanner et al., 2019; Yudovskaya et al., 2013). In contrast, the UCZ typically
426 shows pronounced lithological and compositional variation, consisting of interlayered
427 orthopyroxenite, norite, troctolite, harzburgite, anorthosite and 4-5 major chromitite layers as
428 well as numerous thin chromite stringers. The rocks are relatively evolved (Mg# is typically lower
429 than 0.83), and many contain highly elevated contents of PGE (up to > 10 ppm) and S (up to > 2
430 %)(Maier et al., 2008, 2013; McDonald and Holwell, 2011).

431 *(ii) Lithologies*

432 In general, the studied floor sills are relatively rich in pyroxene and olivine, with plagioclase being
433 less abundant, resulting in the predominance of melanorites, orthopyroxenites, olivine-
434 orthopyroxenites and harzburgites. Gabbronorites are rare, and anorthosites and leuconorites
435 are almost entirely absent. The greatest proportions of mafic rocks, in the form of norites and
436 melanorites, occur at Uitloop II and Amatava, whereas Uitloop I and Rietfontein, as well as the
437 Townlands sills, Bultongfontein and Zwartfontein are predominantly ultramafic.

438 *(iii) Mineral compositions*

439 Few mineral compositional data are available for the studied floor sills. Van der Merwe (1978)
440 found that olivine at Rietfontein has Fo contents between 69 (in troctolite) and 87 (in
441 harzburgite) and that plagioclase in Uitloop I harzburgite has An73. Yudovskaya et al. (2013)
442 provided data on orthopyroxene from Zwartfontein (Mg# 0.82 - 0.88) and Bultongfontein (Mg#
443 0.786 - 0.817). For the current sills, an estimate of Mg# (and An) in the silicate fraction can be
444 obtained via the CIPW norm calculation program (Hollocher, 2004). These data suggest that in all
445 sills Mg# of the silicate fraction reaches values exceeding 0.85. At Uitloop II, average Mg# values
446 are 0.86 for drill core 01-01, 0.89 for drill core 01-03, and 0.86 for drill core 01-05. At Amatava
447 drill core 99-1 has Mg# 0.90 and drill core 99-2 has Mg# 0.87; Uitloop I rocks have Mg# 0.91 and

448 Rietfontein rocks have Mg# 0.87. These data overlap with those of the LZ and LCZ but are less
449 evolved than those of the UCZ (e.g., Maier and Eales, 1997; Maier et al., 2013; McDonald and
450 Holwell, 2011).

451 *(iv) Lithophile whole rock chemistry*

452 The studied sills have 10 - 40 wt.% MgO, 0 - 7 wt.% CaO and 1 - 11 wt.% Al_2O_3, suggesting that
453 the composition of the rocks is controlled mainly by the relative proportions of orthopyroxene,
454 olivine and plagioclase (Figure 11). The major element oxide data show good overlap with both
455 the LZ and LCZ of the WBC. Overlap with the UCZ (including in the northern lobe, i.e. the
456 Platreef) is less good, due to the absence of highly aluminous (feldspathic) lithologies and the
457 significantly lower CaO in the floor sills.

458 In view of the lack of major element data for the Rietfontein body, the latter may be
459 compared to the other sills based on Ni vs Cr relationships (ESM6). These data confirm that
460 Rietfontein is predominantly ultramafic (Ni >500 ppm, Cr >2000 ppm), with mafic rocks being
461 relatively rare and predominantly occurring in the upper portion of the body, as intersected by
462 drill core RF1. The composition of the rocks shows considerable overlap with the LZ and LCZ in
463 the WBC and NBC, and with the ultramafic portions of the Platreef (UCZ) of the northern lobe.
464 However, the Rietfontain body shows less scatter in Ni and Cr contents.

465 The incompatible trace and minor element contents of most of the studied sills (e.g., up
466 to ~100 ppm Zr and 1.2 wt.% K_2O) show good overlap with the UCZ of the northern lobe (i.e. the
467 Platreef and Flatreef) and the B1-UM sills in the floor of the eastern Bushveld (Barnes et al.,
468 2010). In contrast, the CZ and LZ rocks of the northern and western Bushveld typically have
469 significantly lower incompatible trace element contents, with less than ~20 ppm Zr and ~0.2%
470 K_2O (Figure 11c,d).

(v) Sulphur and chalcophile element geochemistry

With the exception of Uitloop I, all studied floor sills contain higher sulphur contents (1000 - 30000 ppm) and PGE contents (typically from 50 ppb to ~3.5 ppm) (Figure 12) than what could be expected in cumulates that crystallised from S-undersaturated Bushveld magma: Assuming a maximum of ~500 ppm S and ~30 ppb Pt+Pd in B1-B3 magmas (Barnes et al. 2010), and trapped melt proportions of 50%, such cumulates would have a maximum of 250 ppm S and 15 ppb Pt+Pd. The studied sills are also mostly enriched in S relative to the LZ and CZ of the WBC but show overlap with the LZ and the Platreef of the Northern lobe (Figure 12). The Rietfontein body, as well as parts of the Uitloop II body (intersected in drill core Uit-03), contain a subset of highly S-enriched samples that lack concomitant PGE enrichment suggesting assimilation of sulphur or sulphide that did not equilibrate with the magma.

The highest PGE concentrations occur in the Uitloop II sill, at up to ~3.5 ppm. The PGE contents of the Uitloop II and Rietfontein bodies show some overlap with the UCZ, except that the latter may have PGE contents in excess of 10 ppm (Figure 12). In contrast, the LZ (and LCZ) of all Bushveld lobes are usually relatively PGE-poor (except for the chromitite seams). However, this could potentially reflect lack of data; Yudovskaya et al. (2013) have identified LZ intervals at Sandspruit and Turfspruit in the northern lobe that may have several 100 ppb PGE, and LZ rocks at the Volspruit deposit have up to ~ 5 ppm PGE (Hulbert and von Gruenewaldt, 1982; Tanner et al., 2019).

Most of the sills have Pt/Pd below unity (Figure 12a, f), overlapping with the lower portions of the Platreef and Flatreef, as well as the LZ, of the northern lobe. The highest Pt/Pd (0.5 - 2) occurs in the Rietfontein sill, showing some overlap with the CZ and LZ of the WBC.

493 The sills mostly have Cu/Pd in the 500 - 3000 range. Compared to primitive mantle
494 (Cu/Pd ~7000), the sills are thus relatively enriched in PGE. In contrast, the UCZ and LZ of the
495 western and northern Bushveld, and the LCZ of the WBC, have highly variable Cu/Pd, with both
496 depleted (Cu/Pd >> 7000=PM) and highly enriched samples (Cu/Pd as low as 20 for some
497 chromitite seams) (Figure 13).

498 In summary, the studied sills show more overlap with LZ or LCZ than with UCZ, notably in
499 terms of Mg# which is higher than in any UCZ rocks. The PGE data are more difficult to evaluate:
500 the studied sills have higher PGE than most LCZ and LZ rocks but lack values of > 5ppm that
501 frequently occur in the UCZ of both the WBC and NBC. In terms of Pt/Pd, there is much better
502 overlap with the NBC than the WBC. Within the NBC, overlap is best with the lower, strongly
503 contaminated portions of the Platreef and Flatreef, suggesting that Pt/Pd is at least partly
504 controlled by contamination.

505

506 Formation of the sulphide mineralisation

507 Magmatic sulphide deposits are normally explained by one of three main models (or a
508 combination thereof): (i) The silicate magma may become saturated in sulphide melt due to
509 fractionation of silicate minerals after final magma emplacement. (ii) The magma may assimilate
510 external S from the floor and/or roof rocks during emplacement. (iii) The magma may have
511 reached sulphide melt saturation prior to final emplacement, in a staging chamber or magma
512 conduit, followed by entrainment of sulphide melt droplets (Naldrett, 2004). In the following
513 section, we assess the relevance of the three models with regard to the formation of the
514 sulphide mineralisation in the northern lobe floor sills.

(i) Magma fractionation after final emplacement

This model is normally employed to explain PGE reefs located within the central portions of some layered intrusions. The model essentially assumes that the parent magma is sulphur-undersaturated during emplacement and thus predicts that fine-grained (chilled) margins observed at the base and roof the intrusions should be sulphur-poor and have higher Cu/Pd than the sulphide-bearing interior of the intrusion. Fine-grained contact rocks occur in the two Amatava drill cores intersecting the Uitloop II body, but these rocks tend to have relatively high sulphur and PGE contents. Thus, there is no evidence that the intruding magmas were sulphide undersaturated. An *in situ* fractionation model for the present sills is also inconsistent with mass balance. The average sulphur contents in those bodies for which complete data coverage is available (drill cores Uit 01-01 and Am 99-1) are 7200 and 4400 ppm, respectively, and average PGE contents are 0.46 ppm and 0.16 ppm, respectively. Bushveld B1 magma has ~500 ppm S (~0.1 % sulphide) and ~30 ppb PGE, thus a closed system fractionation model is not supported by the data.

(ii) Assimilation of external sulphur during emplacement

The earliest models for the formation of sulphide mineralisation in the Platreef of the Bushveld northern lobe invoked *in situ* contamination with sulphidic floor rocks (Wagner, 1929; Barton et al., 1986; Buchanan et al., 1981). The model was based on the abundance of xenoliths and felsic veins, the identification of enriched and variable S, O and Sr isotope ratios and the relatively high proportion of clinopyroxene in the mineralised intervals. Maier et al. (2021b) found that the Flatreef has elevated Cu/Ni relative to the sulphide reefs in the remainder of the Bushveld Complex and argued that the CZ magma in the northern lobe assimilated significant Cu from the floor rocks.

538 Some of the data assembled for the sills studied here clearly suggest crustal
539 contamination, including sulphur isotope data obtained for the Uitloop II body indicating values
540 of $\delta^{34}S$ of +6.6 to +15.3 (Table 3), the presence of pelitic and dolomitic xenoliths (e.g., in drill
541 core Am 99-2), elevated contents of ITE such as K_2O and Zr (drill core Am 99-1), and the presence
542 of Ni-Cu-PGE poor sulphides in drill cores RF6 at Rietfontein and Uit01-03 at Uitloop II. In
543 contrast, CaO/Al_2O_3 ratios, used in a Flatreef study by Maier et al. (2021b) to track assimilation
544 of shale (low CaO/Al_2O_3) vs carbonate (high CaO/Al_2O_3) are in the range of typical noritic and
545 pyroxenitic cumulates, i.e. show no evidence of contamination in the studied sills (ESM6).
546 Equally, we see no correlation between concentrations of PGE and incompatible lithophile
547 elements (Zr, K_2O), and thus there is no indication that any contamination caused the sulphide
548 mineralisation. Another problem with the *in situ* contamination model is that this normally
549 results in the highest sulphur contents and PGE grades near the base of intrusions, contrary to
550 some of the present sills. We conclude that contamination was unlikely to be the only or most
551 important mechanism to cause the PGE mineralisation in the sills.

552 *(iii) Entrainment of sulphides that formed prior to final magma emplacement*

553 Several authors have proposed that the Bushveld floor sills formed by ejection of
554 magmas from the Bushveld main magma chamber, perhaps in response to tectonic adjustments
555 or cumulate compaction (Sharpe and Hulbert 1985; Yao et al. 2021). If the cumulates in the main
556 chamber were sulphide-rich (e.g., the Platreef), this model could result in the formation of
557 sulphidic floor sills. However, in that case one would expect that the sulphides in the sills have
558 broadly similar compositions as the Platreef sulphides. This is only partly true: The sills do have
559 Pt and Pd contents (up to 3 ppm) and Pt+Pd tenors (10-40 ppm) as well as Pt/Pd ratios (mostly
560 below unity) resembling those in the lower parts of the Platreef. However, Cu/Ni in the sills is

much lower than in Platreef rocks with similar MgO contents (Figure 12c). This implies that the magma from which the sills crystallised was not derived from the Platreef.

One could consider formation of the footwall sills via ejection of LZ magma (Sharpe & Hulbert, 1985; Yao et al., 2021). However, the margins of the present floor sills, as well as those below the EBC (Sharpe, 1981) tend to be relatively sharp and quenched, suggesting that the floor was relatively cold during sill emplacement, inconsistent with magma derivation from a large proximal magma chamber.

Entrainment of sulphides from a staging chamber or feeder conduit could potentially explain the pronounced sulphide and PGE enrichment of most of the studied floor sills. The model was previously suggested for the Platreef (Barton et al., 1986; Harris and Chaumba, 2001; Hutchinson and Kinnaird, 2005; McDonald and Holwell, 2007; Holwell and McDonald, 2007; Ihlenfeld and Keays, 2011; Mitchell and Scoon, 2012; Scoon et al., 2020; Beukes et al., 2020). Holwell et al. (2011) reported on PGE-rich sulphide melt inclusions in chromite grains. Arguing that the chromites were the first minerals to crystallise from the magma the authors implied that the magma was saturated in sulphide melt prior to final emplacement. However, chromite tends to anneal (Eales and Reynolds, 1986) and can form during late magmatic recrystallisation of cumulates (Boudreau, 2019; Mathez and Kinzler, 2017). The key evidence for sulphide entrainment from depth would comprise aphyric, sulphide-enriched dykes or sills in the floor of an intrusion that could represent parent liquids. No such dykes or sills have yet been identified in the floor of the Bushveld Complex; In fact, all the fine-grained floor sills studied by Sharpe (1981) and Barnes et al. (2010) are undersaturated in S and have PGE contents broadly in the range of normal basalts. Another challenge to the model of sulphide entrainment from a deeper staging chamber or magma conduit is that all the Bushveld mineralised intrusives (i.e. the Platreef,

584 Flatreef, Uitkomst and some of the sills studied here) are hosted by the Duitschland Foration and
585 Malmani Subgroup. This suggests a strong host rock control on the mineralisation, consistent
586 with the available sulphur isotope data (Sharman Harris et al., 2013, and Table 3).

587 We conclude that the currently available evidence is inconsistent with sulphide
588 entrainment from a deeper staging chamber or magma conduit. However, the high sulphide
589 budget of many of the studied sills suggests that they formed as open systems, with sulphides
590 precipitating from magma passing through the sills. This implies that the magma was S saturated
591 during emplacement, which in turn implies that sulphides were entrained locally, during sill
592 propagation within the Malmani Subgroup and Duitschland Formation which together can be up
593 to 3 km thick (Bekker et al., 2001). This model was first proposed by Sharman Harris et al. (2013)
594 based on sulphur isotope data, and it is consistent with the relatively constant Mg# at, e.g.,
595 Amatava.

596 Towards a refined ore model for the Bushveld floor sills

597 *(i) Shape and size of intrusions* – The best Ni-Cu-PGE sulphide targets appear to be sills
598 that show evidence for magma throughflow (e.g., in the form of constant Mg#). Such magma
599 feeder conduits favour entrainment of sulphides, causing relatively high R factors (mass ratio of
600 silicate magma to sulphide melt, Fig. 13) and sulphide concentration in flow dynamic traps
601 (Naldrett, 2004; Barnes et al., 2016). The most highly mineralised sill (Uitkomst, located near
602 Badplaas in the floor of the southeastern Bushveld Complex) is relatively thick (~1 km), likely
603 resulting in particularly high heat flux, crustal assimilation, and slow cooling, all of which may
604 facilitate sulphide concentration via prolonged sulphide melt percolation through semi-
605 consolidated cumulates (Maier et al., 2018).

606 *(ii) Location of intrusions* – Mineralised floor sills have been located below the NBC and
607 EBC, including those studied in the present work, as well as at Uitkomst (Gauert et al., 1998) and
608 Helvetia (Maier et al., 2001), but most occur to the north of Mokopane. The Mokopane area also
609 hosts unusually Mg-, S- and chromite rich LZ, namely at Grasvalley (Hulbert and von
610 Gruenewaldt, 1982). To the SW of Mokopane occurs the largest positive gravity anomaly in the
611 Bushveld, interpreted as a major magma feeder zone (Finn et al., 2015; Cole et al., 2021). Such
612 environments are typically characterised by enhanced heat flux, favouring contamination with
613 the country rocks. Magma feeder conduits tend to be associated with swarms of sills and dykes,
614 e.g., at mid-ocean ridges or in sill sediment complexes (Magee et al., 2016). However, few of
615 these settings appear to host orebodies, serving as a reminder that ore formation depends on a
616 range of processes, as discussed below.
617 *(iii) Host rocks to intrusions/ contamination:* Most mineralised intrusions in the floor of
618 the Bushveld Complex have been emplaced within the lower portion of the Transvaal
619 Supergroup, notably the Duitschland Formation and Malmani Subgroup, constituting preferential
620 horizons for magma injection (e.g., Hutton, 2009). Based on the occurrence of the richest
621 Platreef associated with Malmani dolomite at Sandsloot, De Waal (1977) suggested that
622 dolomitic country rocks are key in the formation of massive Ni-Cu-PGE ores. The idea was that
623 H_2O and CO_2 addition cause magma oxidation and thus sulphide melt saturation. It has since
624 been demonstrated that oxidation stabilizes sulfate and thus increases the S content at sulphide
625 saturation in the magma (Jugo et al., 2005), possibly delaying sulphide melt saturation (Iacono-
626 Marciano et al., 2017). However, if initial oxidation is followed by reduction (e.g., via assimilation
627 of organic-rich shale) this may reduce the magma sufficiently to result in sulphide melt
628 saturation, as, e.g., proposed for Norilsk (Iacono-Marciano et al., 2017). The model is particularly
629 attractive in the Bushveld province, being that the Transvaal Supergroup sedimentary rocks

underlying much of the northern limb comprise a basal unit of dolomite (the Malmani Subgroup) containing locally sulfate (Kesler et al., 2007; Gandin et al., 2005). Assimilation of these rocks could increase the S content of the magma, whereas graphite and anhydrite- bearing shale of the Duitschland Formation that overlies the Malmani Subgroup (Yudovskaya et al., 2021) could trigger sulphide melt saturation.

The association of the highest-grade sulphides with Malmani dolomite, in the Platreef and at Uitkomst, could be explained by relatively enhanced magmatic erosion of the dolomite (Maier et al., 2018). If this model is correct, the Malmani dolomite may constitute a critical trap within the Bushveld mineral system, as originally envisaged by de Waal (1977). Sills that have been emplaced below or above this "productive interval" (in reference to the "productive sedimentary pile" of the Pechenga belt, Hanski, 1992) of the Malmani Subgroup-Duitschland Formation appear to be much less prospective. This includes Uitloop I which has been emplaced into relatively sterile Archaean basement, and the low-grade mineralized Helvetia sills on the farm Blaauwboschkraal, emplaced into Silverton shale in the floor of the EBC (Maier et al. 2001).

(iv) Reactive porous flow: Experiments have shown that degassing of sulphide melt may produce metal-enriched sulphide melts and, ultimately, PGMs (Iocono-Marciano et al., 2020, 2022). This model could be applied to the S-poor, PGE enriched Rietfontein cumulates which could have formed through late magmatic degassing of cumulates partially dissolving magmatic sulphides, consistent with the relatively high Pt/Pd of the rocks.

Unresolved aspects of the Bushveld mineral system

(i) Relative timing of magma surges; In some magmatic provinces, it has been shown that strongly sulphide mineralised intrusions represent early magma pulses (e.g., Nebo Babel, Kunene, Munali). Such early magma surges could interact with relatively fertile,

654 unmetamorphosed crust, whereas contamination of late magma surges could be impeded by the
655 crystallization products of earlier surges lining the magma conduits. This model could potentially
656 explain why the WBC and EBC cumulates do not show evidence of sulphide extraction even
657 though their parent magmas must have interacted with the Duitschland Formation at depth (Fig.
658 14A). Sulphide saturation was ultimately reached upon final emplacement via fractionation,
659 resulting in the reef-type deposits.

660 (ii) Crustal stress regime; Research on porphyry systems suggests that ore deposits may
661 form during the transition from one stress regime to the other (Chelle-Michou and Rottier,
662 2021). Predominantly extensional regimes may be represented by dykes whereas compressional
663 regimes are represented by sills. In the context of magmatic deposits, there is some evidence
664 that mineralised dykes (e.g., Voisey's Bay, Eagle) are rarer and less mineralised than sills (e.g.,
665 Nebo Babel, Norilsk, Kabanga, Uitkomst), perhaps because dykes reflect large, but dispersed
666 magma flux whereas sills reflect more focused magma flux favoring assimilation of crust and
667 flow dynamic concentration of sulphides. One should target periods in the evolution of a
668 province characterised by high magma flux, but also a switch in the stress regime from
669 extensional to compressional or transtensional, causing the magma to bottle up and focus. A
670 complication is that there is unlikely to be a clear distinction between early extensional and late
671 compressional regimes. Regimes could switch and revert at any stage, e.g., when different
672 portions of the crust behave differently during extension or compression, causing temporary
673 bottling up and release at any stage during the evolution of a province. This could explain the
674 occurrence of both early (e.g., Nebo, Munali) and relatively late mineralised conduits (e.g.,
675 Uitkomst).

(iii) Enhanced mineralisation potential of the UCZ; Both the Platreef and the LZ locally intrude Duitschland Formation and thus should have had the opportunity to assimilate external sulphide, yet the LZ is apparently unprospective. Possibly, the LZ could be underexplored, or it is more S-undersaturated than the CZ due to its less evolved composition, or the LZ could represent a late phase intruding into metamorphosed floor (Scoates et al., 2021).

Conclusions

The northern limb of the Bushveld Complex is underlain by several floor sills. The sills are of interest for exploration as they could constitute feeder conduits to the intrusion and as such might host economic Ni-Cu-PGE sulphide mineralization. In the present study we have reviewed exploration assay data for a number of sills on the farms Townlands, Uitloop, Amatava and Rietfontein, complemented by new whole rock data on lithophile and chalcophile element contents and sulphur isotopes. The sills consist of orthopyroxenite, harzburgite and norite, emplaced into the basal portion of the Transvaal Supergroup (Duitschland and Malmani formations) and the Archaean granite-gneiss basement. Many of the sills contain PGE-rich sulphides, particularly in the pyroxenitic portions which locally host up to ~3 ppm PGE. Sulphide melt saturation was likely reached due to contamination, as suggested by the presence of xenoliths as well as compositional data, including sulphur isotopes ($\delta^{34}S$ +7 to +15). Relatively high metal tenors require R factors on the order of 1000-10000, suggesting that the sulphides were upgraded during entrainment within the sills. The high abundance of the sills in the vicinity of the Mokopane gravity high suggests that Ni-Cu-PGE prospectivity is in part controlled by proximity to magma feeder zones. As yet, no economic mineralization has been encountered, but relatively few boreholes have been drilled and grade is highly variable along strike.

699 Heterogenous sulphide distribution is characteristic of many conduit-hosted sulphide deposits,
700 suggesting that there remains potential for further exploration.
701
702 **Acknowledgements**
703 John Blaine is thanked for providing historic exploration assays from Falconbridge Ventures of
704 Africa. Our interpretations benefitted from discussions with Steve Barnes. Marina Yudovskaya,
705 Giada Iacono-Marziano and an anonymous reviewer provided constructive reviews.
706
707
708 **References**
709 Barnes, S.J., Cruden, A.R., Arndt, N. and Saumur, B.M., 2016. The mineral system approach
710 applied to magmatic Ni–Cu–PGE sulphide deposits. Ore Geology Reviews, 76, 296-316.
711
712 Barnes, S-J., Maier, W.D. and Curl, E., 2010. Composition of the Marginal Rocks and Sills of the
713 Rustenburg Layered Suite, Bushveld Complex, South Africa: Implications for the Formation of the
714 Platinum -Group Element Deposits. Economic Geology, 105, 1481-1511.
715
716 Barton, J.M., Cawthorn, R.G. and White, J.A., 1986. The role of contamination in the evolution of
717 the Platreef of the Bushveld Complex. Economic Geology, 81, 1096–1108.
718
719 Bekker, A., Kaufman, A.J., Karhu, J.A., Beukes, N.J., Swart, Q.D., Coetzee, L.L. and Eriksson, K.A.,
720 2001. Chemostratigraphy of the Paleoproterozoic Duitschland Formation, South Africa:
721 implications for coupled climate change and carbon cycling. American Journal of Science, 301(3),
722 261-285.

723

724 Bennett, H. and Oliver, G., 1992. XRF Analysis of Ceramics. Minerals and applied materials. John
725 Wiley and Son, New York. United States of America. 67-93.

726

727 Beukes, J.J., Roelofse, F., Gauert, C.D.K., Grobler, D.F. and Ueckermann, H., 2021. Strontium
728 isotope variations in the Flatreef and its immediate footwall and hanging wall on Macalakaskop,
729 Northern Limb, Bushveld Complex. Mineralium Deposita, 56, 45-57.

730

731 Boudreau, A., 2019. Hydromagmatic processes and platinum-group element deposits in layered
732 intrusions. Cambridge University Press, 275 pp.

733

734 Buchanan, D.L., Nolan, J., Suddaby, P., Rouse, J.E., Viljoen, M.J., and Davenport, J.W.J., 1981. The
735 genesis of sulfide mineralization in a portion of the Potgietersrus limb of the Bushveld Complex.
736 Economic Geology, 76, 568–579.

737

738 Cawthorn, R.G., Barton, J.R. and Viljoen, M.J., 1985. Interaction of floor rocks with the Platreef
739 on Overysel, Potgietersrus, northern Transvaal. Economic Geology, 80, 988–1006.

740

741 Chung, H.Y. and Mungall, J.E., 2009. Physical constraints on the migration of immiscible fluids
742 through partially molten silicates, with special reference to magmatic sulfide ores. Earth and
743 Planetary Science Letters, 286(1-2), 14-22.

744

745 Cole, J., Finn, C.A. and Webb, S.J., 2021. Geometry of the Bushveld Complex from 3D potential
746 field modelling. Precambrian Research, 359, 106219.

747

748 Eales, H.V. and Reynolds, I.M., 1986. Cryptic variations within chromitites of the upper critical
749 zone, northwestern Bushveld Complex. Economic Geology, 81, 1056-1066.

750

751 Finn, C.A., Bedrosian, P.A., Cole, J.C., Khoza, T.D. and Webb, S.J., 2015. Mapping the 3D extent of
752 the Northern Lobe of the Bushveld layered mafic intrusion from geophysical data. Precambrian
753 Research, 268, 279-294.

754

755 Gandin, A., Wright, D.T. and Melezhik, V., 2005. Vanished evaporites and carbonate formation in
756 the Neoarchaean Kogelbeen and Gamohaan formations of the Campbellrand Subgroup, South
757 Africa. Journal of African Earth Sciences, 41(1-2), 1-23.

758

759 Gauert, C.D.K., De Waal, S.A. and Wallmach, T., 1995. Geology of the ultrabasic to basic Uitkomst
760 Complex, eastern Transvaal, South Africa: an overview. Journal of African Earth Sciences, 21(4),
761 553-570.

762

763 Grobler, D.F., Brits, J.A.N., Maier, W.D. and Crossingham, A., 2019. Litho- and chemostratigraphy
764 of the Flatreef PGE deposit, northern Bushveld Complex, Mineralium Deposita, DOI
765 10.1007/s00126-012-0436-1

766

767 Hanski, E.J., 1992. Petrology of the Pechenga ferropicrites and cogenetic, Ni-bearing gabbro-
768 wehrlite intrusions, Kola Peninsula, Russia. Geological Survey of Finland Bulletin, 367, 192pp.

769

770 Harris, C. and Chaumba, J.B., 2001. Crustal contamination and fluid–rock interaction during the
771 formation of the Platreef, northern limb of the Bushveld Complex, South Africa. Journal of
772 Petrology, 42, 1321–1347.
773
774 Hollocher, K., 2004. CIPW Norm Calculation Program. Geology Department, Union College, USA.
775
776 Holwell, D.A. and McDonald, I., 2007. Distribution of platinum-group elements in the Platreef at
777 Overysel, northern Bushveld Complex: a combined PGM and LA-ICP-MS study. Contributions to
778 Mineralogy and Petrology, 154, 171–190.
779
780 Holwell, D.A. and Jordaan, A., 2006. Three-dimensional mapping of the Platreef at the
781 Zwartfontein South mine: implications for the timing of magmatic events in the northern limb of
782 the Bushveld Complex, South Africa. Applied Earth Science, 115, 41-48.
783
784 Holwell, D.A., McDonald, I. and Butler, I.B., 2011. Precious metal enrichment in the Platreef,
785 Bushveld Complex, South Africa: evidence from homogenized magmatic sulfide melt inclusions.
786 Contributions to Mineralogy and Petrology, 161, 1011-1026.
787
788 Hulbert, L.J. and Von Gruenewaldt, G., 1982. Nickel, copper, and platinum mineralization in the
789 lower zone of the Bushveld Complex, south of Potgietersrus. Economic Geology, 77, 1296-1306.
790
791 Hutchinson, D. and Kinnaird, J.A., 2005. Complex multistage genesis for the Ni–Cu–PGE
792 mineralisation in the southern region of the Platreef, Bushveld Complex, South Africa. Applied
793 Earth Science, 114, 208-224.

794

795 Hutton, D.H.W., 2009. Insights into magmatism in volcanic margins: bridge structures and a new
796 mechanism of basic sill emplacement–Theron Mountains, Antarctica. Petroleum Geoscience, 15,
797 269-278.

798

799 Ihlenfeld, C. and Keays, R.R., 2011. Crustal contamination and PGE mineralization in the Platreef,
800 Bushveld Complex, South Africa: evidence for multiple contamination events and transport of
801 magmatic sulfides. Mineralium Deposita, 46, 813-832.

802

803 Iacono-Marziano, G., Ferraina, C., Gaillard, F., Di Carlo, I. and Arndt, N.T., 2017. Assimilation of
804 sulfate and carbonaceous rocks: Experimental study, thermodynamic modeling and application
805 to the Noril'sk-Talnakh region (Russia). Ore Geology Reviews, 90, 399-413.

806

807 Iacono-Marziano, G., Le Vaillant, M., Godel, B.M., Barnes, S.J. and Arbaret, L., 2022. The critical
808 role of magma degassing in sulphide melt mobility and metal enrichment. Nature
809 Communications, 13, 1-10.

810

811 Kesler, S.E., Reich, M. and Jean, M., 2007. Geochemistry of fluid inclusion brines from Earth's
812 oldest Mississippi Valley-type (MVT) deposits, Transvaal Supergroup, South Africa. Chemical
813 Geology, 237, 274-288.

814

815 Kinnaird, J. A. and McDonald, I., 2018. The northern limb of the Bushveld Complex: a new
816 economic frontier. Society of Economic Geologists Special Publication, 21, 157-176.

817

818 Kinnaird, J.A., Hutchinson, D., Schurmann, L., Nex, P.A.M. and de Lange, R., 2005. Petrology and
819 mineralization of the southern Platreef: northern limb of the Bushveld Complex, South Africa.
820 Mineralium Deposita, 40, 576-597.
821
822 Lesher, C.M. and Burnham, O.M., 2001. Multicomponent elemental and isotopic mixing in Ni–
823 Cu–(PGE) ores at Kambalda, Western Australia. The Canadian Mineralogist, 39, 421-446.
824
825 Magee, C., Muirhead, J.D., Karvelas, A., Holford, S.P., Jackson, C.A., Bastow, I.D., Schofield, N.,
826 Stevenson, C.T., McLean, C., McCarthy, W. and Shtukert, O., 2016. Lateral magma flow in mafic
827 sill complexes. Geosphere, 12, 809-841.
828
829 Maier, W.D. and Eales, H.V., 1997. Correlation within the UG2-Merensky Reef interval of the
830 Western Bushveld Complex, based on geochemical, mineralogical and petrological data. Bulletin
831 20. Council for Geoscience: 56pp
832
833 Maier, W.D., Sliep, J., Barnes, S.J., De Waal, S.A. and Li, C., 2001. PGE-bearing mafic-ultramafic
834 sills in the floor of the eastern Bushveld Complex on the farms Blaauwboschkraal, Zwartkopje,
835 and Waterval. South African Journal of Geology, 104, 343-354.
836
837 Maier, W.D., de Klerk, L., Blaine, J., Manyeruke, T., Barnes, S-J., Stevens, M.V.A. and Mavrogenes
838 J.A., 2008. Petrogenesis of contact-style PGE mineralization in the northern lobe of the Bushveld
839 Complex: comparison of data from the farms Rooipoort, Townlands, Drenthe and Nonnenwerth.
840 Mineralium Deposita, 43, 255-280.
841

842 Maier, W.D., Barnes, S-J. and Groves, D.I., 2013. The Bushveld Complex, South Africa: Formation
843 of platinum-palladium, chrome and vanadium- rich layers via hydrodynamic sorting of a
844 mobilized cumulate slurry in a large, relatively slowly cooling, subsiding magma chamber.
845 Mineralium Deposita, 48, 1-56.
846
847 Maier, W.D., Yudovskaya, M. and Jugo, P., 2021. Introduction to the special issue on the Flatreef
848 PGE-Ni-Cu deposit, northern limb of the Bushveld Igneous Complex. Mineralium Deposita, 56, 1-
849 10.
850
851 Maier, W.D., Abernethy, K.E.L., Grobler, D.F. and Moorhead, G., 2021. Formation of the Flatreef
852 deposit, northern Bushveld, by hydrodynamic and hydromagmatic processes. Mineralium
853 Deposita, 56, 11-30.
854
855 Manyeruke, T., Maier, W.D., Barnes, S-J., 2005. Major and trace element geochemistry of the
856 Platreef on the farm Townlands, northern Bushveld Complex. South African Journal of Geology,
857 108, 379–394.
858
859 Mathez, E.A. and Kinzler, R.J., 2017. Metasomatic chromitite seams in the Bushveld and Rum
860 layered intrusions. Elements, 13, 397-402.
861
862 McCuaig, T.C., Beresford, S. and Hronsky, J., 2010. Translating the mineral systems approach into
863 an effective exploration targeting system. Ore Geology Reviews, 38, 128-138.
864

McDonald, I. and Holwell, D.A., 2007. Did lower zone magma conduits store PGE-rich sulphides that were later supplied to the Platreef? South African Journal of Geology, 110, 611-616.

McDonald, I. and Holwell, D.A., 2011. Geology of the northern Bushveld Complex and the setting and genesis of the Platreef Ni-Cu-PGE deposit. Reviews in Economic Geology, 17, 297-327.

Mitchell, A.A., Scoon, R.N., 2012. The Platreef of the Bushveld Complex, South Africa: a new hypothesis of multiple, non-sequential magma replenishment based on observations at the Akanani Project, north-west of Mokopane. South African Journal of Geology, 115, 535-550.

Mungall, J.E. and Brenan, J.M., 2014. Partitioning of platinum-group elements and Au between sulfide liquid and basalt and the origins of mantle-crust fractionation of the chalcophile elements. Geochimica et Cosmochimica Acta, 125, 265-289.

Naldrett, A.J. and Naldrett, A.L., 2004. Magmatic sulfide deposits: geology, geochemistry and exploration. Springer Science & Business Media. 728 pp.

Naldrett, A.J., Wilson, A., Kinnaird, J., Chunnett, G., 2009. PGE tenor and metal ratios within and below the Merensky Reef, Bushveld Complex: implications for its genesis. Journal of Petrology, 50, 625-659.

Richardson, S.H. and Shirey, S.B., 2008. Continental mantle signature of Bushveld magmas and coeval diamonds. Nature, 453, 910-913.

889 Scoates, J.S., Wall, C.J., Friedman, R.M., Weis, D., Mathez, E.A. and VanTongeren, J.A., 2021.
890 Dating the Bushveld Complex: timing of crystallization, duration of magmatism, and cooling of
891 the world's largest layered intrusion and related rocks. Journal of Petrology, 62,
892 https://doi.org/10.1093/petrology/egaa107
893
894 Scoon, R.N. and Teigler, B., 1994. Platinum-group element mineralization in the critical zone of
895 the western Bushveld Complex; I, Sulfide poor-chromitites below the UG-2. Economic Geology,
896 89, 1094-1121.
897
898 Scoon, R.N., Costin, G., Mitchell, A.A. and Moine, B., 2020. Non-sequential injection of PGE-rich
899 ultramafic sills in the Platreef Unit at Akanani, Northern Limb of the Bushveld Complex: Evidence
900 from Sr and Nd isotopic systematics. Journal of Petrology, 61, doi: 10.1093/petrology/egaa032
901
902 Sharman Harris, E.R., Penniston-Dorland, S.C., Kinnaird, J.A., Nex, P.A.M., Brown, M., Wing, B.A.,
903 2013. Primary origin of marginal Ni-Cu-(PGE) mineralization in layered intrusions: Δ33S evidence
904 from The Platreef, Bushveld, South Africa. Economic Geology, 108, 365-377.
905
906 Sharpe, M.R., 1981. The chronology of magma influxes to the eastern compartment of the
907 Bushveld Complex as exemplified by its marginal border groups. Journal of the Geological
908 Society, 138, 307-326.
909
910 Sharpe, M.R. and Hulbert, L.J., 1985. Ultramafic sills beneath the eastern Bushveld Complex;
911 mobilized suspensions of early lower zone cumulates in a parental magma with boninitic
912 affinities. Economic Geology, 80, 849-871.

913

914 Stephenson, H., 2018. The Platreef magma event at the world-class Turfspruit Ni-Cu-PGE deposit:
915 implications for mineralisation processes and the Bushveld Complex stratigraphy (Doctoral
916 dissertation, Cardiff University), 454 pp.

917

918 Tanner, D., McDonald, I., Harmer, R.J., Muir, D.D. and Hughes, H.S., 2019. A record of
919 assimilation preserved by exotic minerals in the lowermost platinum-group element deposit of
920 the Bushveld Complex: The Volspruit Sulphide Zone. Lithos, 324, 584-608.

921

922 Teigler, B. and Eales, H.V., 1996. The Lower and Critical Zones of the western limb of the
923 Bushveld Complex as intersected by the Nooitgedacht boreholes. Bulletin of the Geological
924 Survey of South Africa, Vol. 111, Council for Geoscience, 126 pp.

925

926 Van der Merwe, M.J., 1976. The layered sequence of the Potgietersrus limb of the Bushveld
927 Complex. Economic Geology, 71, 1337-1351.

928

929 van der Merwe, M.J., 1978. The Geology of the basic and ultramafic rocks of the Potgietersrus
930 Limb of the Bushveld Complex: Unpublished Ph. D (Doctoral dissertation, thesis, University of
931 Witwatersrand), 176 pp.

932

933 Wagner, P.A., 1929. The platinum deposits of the Bushveld Complex. Oliver and Boyd, Edinburgh,
934 588pp.

935

936 Watson, J.S., 1996. Fast, simple method of powder pellet preparation for X-ray fluorescence
937 analysis. X-Ray Spectrometry, 25, 173-174.
938
939 Yao, Z., Mungall, J.E. and Jenkins, M.C., 2021. The Rustenburg Layered Suite formed as a stack of
940 mush with transient magma chambers. Nature Communications, 12, 1-13.
941
942 Yudovskaya, M.A., Kinnaird, J.A., Sobolev, A.V., Kuzmin, D.V., McDonald, I. and Wilson, A.H.,
943 2013. Petrogenesis of the Lower Zone olivine-rich cumulates beneath the Platreef and their
944 correlation with recognized occurrences in the Bushveld Complex. Economic Geology, 108, 1923-
945 1952.
946
947 Yudovskaya, M., Belousova, E., Kinnaird, J., Dubinina, E., Grobler, D.F., Pearson, N., 2017. Re-Os
948 and S isotope evidence for the origin of Platreef mineralization (Bushveld Complex). Geochimica
949 et Cosmochimica Acta, 214, 282-307.
950
951 Yudovskaya, M.A., Sluzhenikin, S.F., Costin, G., Shatagin, K.N., Dubinina, E.O., Grobler, D.F.,
952 Ueckermann, H. and Kinnaird, J.A., 2018. Anhydrite assimilation by ultramafic melts of the
953 Bushveld Complex, and its consequences to petrology and mineralization. Society of Economic
954 Geologists Special Publications, 21, 177–206.
955
956 Yudovskaya, M.A., Costin, G., Sluzhenikin, S.F., Kinnaird, J.A., Ueckermann, H., Abramova, V.D.
957 and Grobler, D.F., 2021. Hybrid norite and the fate of argillaceous to anhydritic shales
958 assimilated by Bushveld melts. Mineralium Deposita, 56, 73-90.
959

960

961

962

963

964

965 **Figures**

966 Figure 1: (a) Geological locality map of study area. The metamorphosed sediments of the upper
967 Pretoria Group consist of undifferentiated quartzite of the Magaliesberg Formation, as well as
968 shale and hornfels (and minor amounts of marble and calc-silicate) of the Timeball Hill
969 Formation. The lower Pretoria Group is represented by the intercalated shale, dolomite and
970 minor quartzite beds of the Duitschland Formation. (b) High resolution VRMI image of study
971 area, overlain on the regional TMI image. The Total Magnetic Intensity (TMI) shows the magnetic
972 field as it is at the time of the survey with information about susceptibility contrast, remanence,
973 and structure. However, conventional TMI hides many lineaments because of dynamic range and
974 inclusion of all remanent magnetisation. Vector Remanent Magnetic Intensity (VRMI) is the
975 amplitude of the total magnetisation of the earth with no vector components. By eliminating the
976 effect of remanence, all magnetic anomalies with their respective dips, strikes and depths are
977 shown in their correct location, as can be seen for the Amatava, Townlands and Uitloop drill
978 targets. Ultramafic rock units are clearly visible as linear, highly magnetic anomalies on the TMI
979 image. The Dolerite dykes, banded iron formation and bedding orientation of the intercalated
980 sedimentary rocks can also be identified in the VRMI image.

981

982 Figure 2: (a) Block model of Uitloop II intrusion. (b) Drill core logs of the Uitloop II body.
983 D=Duitschland Formation; P=Penge Iron Formation; M=Malmani Subgroup. Numbers to left of
984 columns denote meters below collar of boreholes.

985

986 Figure 3: Binary variation plots of (a) Pt+Pd and (b) Ni plotted vs S in drill core Uit 01-01.

987

988 Figure 4: Compositional data from drill core Uit01-01, plotted vs height (in metres below
989 borehole collar). Px=pyroxenite, No=norite, Hy=hybrid rock of norite and diamictite.

990

991 Fig. 5: Compositional data from drill core Am99-2, plotted vs height (in metres below borehole
992 collar).

993

994 Figure 6: Compositional variation in drill core Am99-01, plotted vs stratigraphic height (in metres
995 below borehole collar).

996

997 Figure 7: Compositional variation of Uitloop I body. (A) Binary variation diagram of CaO vs Al_2O_3,
998 showing homogeneity of orthopyroxenites and paucity of plagioclase and clinopyroxene. Insert
999 shows close-up of data distribution near orthopyroxene end-member composition. (B) Plot of Cr
1000 vs MgO. Western Bushveld Complex data from Teigler and Eales (1996) and Turfspruit LZ data
1001 from Yudovskaya et al. (2013). EBC = eastern Bushveld Complex; NBC = northern Bushveld
1002 Complex.

1003

1004 Figure 8: Photographs of Rietfontein intrusions. (A) Interlayered harzburgite, olivine pyroxenite
1005 and pyroxenite in drill core RF2. Depth interval = 46.3 m to 59.2 m. Note sharp lower contact and
1006 gradational upper contact of poikilitic harzburgite layer. Harzburgite at 54-55 m has 2375 ppm
1007 Ni, 3885 ppm Cr, 105 ppm Cu, 400 ppm S, and 70 ppb Pt+Pd. In contrast, orthopyroxenite at 48-
1008 49 m has 820 ppm Ni, 2850 ppm Cr, 300 ppm S, and 70 ppb PGE. (B) strongly altered and felsic
1009 veined pyroxenite in drill core RF5, 603.09 m – 611 m. Rock has 600 ppm Ni, 2000 ppm Cr, 30
1010 ppm Cu, < 0.01 wt % S, 0.3 ppm PGE. (C) Foliated pyroxenite in drill core RF6, 176 m, with ~760
1011 ppm Ni, 4000 ppm Cr, 40 ppm Cu and 0.04 ppm PGE.

1012 Figure 9: Binary variation plots of selected metal data in Rietfontein rocks. (a) Ni vs Cr, (b) Ni vs
1013 Pt+Pd, (c) Pt/Pd vs Pt+Pd, (d) S vs Pt+Pd. Note PGE enrichment predominantly in relatively S-poor
1014 lithologies that have < 1000 ppm Ni, i.e., likely represent pyroxenite and norite.

1015

1016 Figure 10: Assay data from drill core RF6. Note that borehole was drilled vertically and thickness
1017 of intervals does not represent true thickness. Depth is given in in metres below borehole collar.

1018

1019 Figure 11: Binary variation diagrams showing composition of analysed rocks in comparison to LZ
1020 and UCZ of WBC (data from Maier et al., 2013). (a) Al_2O_3 vs MgO. Rocks are controlled by
1021 variable proportions of plagioclase, olivine, orthopyroxene and clinopyroxene. Note that
1022 Platreef, Flatreef and UCZ in WBC may contain leuco(gabbro)noritic and anorthositic rocks,
1023 whereas floor sills are predominantly ultramafic or mela (gabbro)noritic. (b) CaO vs MgO. While
1024 footwall sills are largely controlled by plagioclase-olivine and orthopyroxene, many Platreef and

1025 Flatreef rocks additionally contain significant clinopyroxene. (c) Zr vs MgO, (d) K_2O vs MgO. Note
1026 broad overlap of present sills with many Platreef/Flatreef rocks, but generally lower
1027 concentrations in LZ and UCZ of WBC.

1028

1029 Figure 12: Binary variation plots of Pt+Pd and Pt/Pd vs S. Note that data overlap with LCZ and LZ,
1030 but there are also some unusually S rich, yet PGE poor samples that likely represent external S
1031 addition at a late- or post-magmatic stage (at Rietfontein and in drill core Uit01-03)

1032

1033 Figure 13: Plot of Cu/Pd vs Pd for samples from across the Bushveld Complex. Composition of B1
1034 is from Barnes et al. (2010). Tie lines are mixing lines between B1 silicate melt and sulphide melt
1035 segregating at various R factors. Note that UCZ and LZ from WBC have both enriched and
1036 depleted samples, with the former indicating relatively high R factors. Many Platreef and Flatreef
1037 samples show depleted Cu/Pd > 7000 which has been explained by addition of Cu from the floor
1038 rocks (Maier et al., 2021b). Considering this, the R factors applicable are in the range 100-1000.
1039 The footwall sills have intermediate R factor (1000-10000), but their observed sulphide contents
1040 are lower than in the model, possibly due to addition of sedimentary S that could not equilibrate
1041 with the magma. The Rietfontein body has mostly enriched signatures, with high R factors,
1042 overlapping with the UCZ and LZ of the WBC.

1043

1044 Figure 14: (A) Sketch model of Bushveld Complex, showing broadly concordant relationship to
1045 floor rocks in WBC and EBC, but transgressive relationship in NBC. TML= Thabazimbi-Murchison
1046 Lineament. Solid black/grey lines indicate putative unprospective B1/B2 dykes and sills. Red

lines/polygons indicate sulphide enriched (prospective) sills below Bushveld and contact-style deposits within main Bushveld Complex. Prospectivity of sills is proposed to decrease with distance from feeder zone, indicated by colour change from red to pink and white. Stippled red line indicates internal reefs. (B) Gravity model of Bushveld Complex (from Cole et al. 2014).

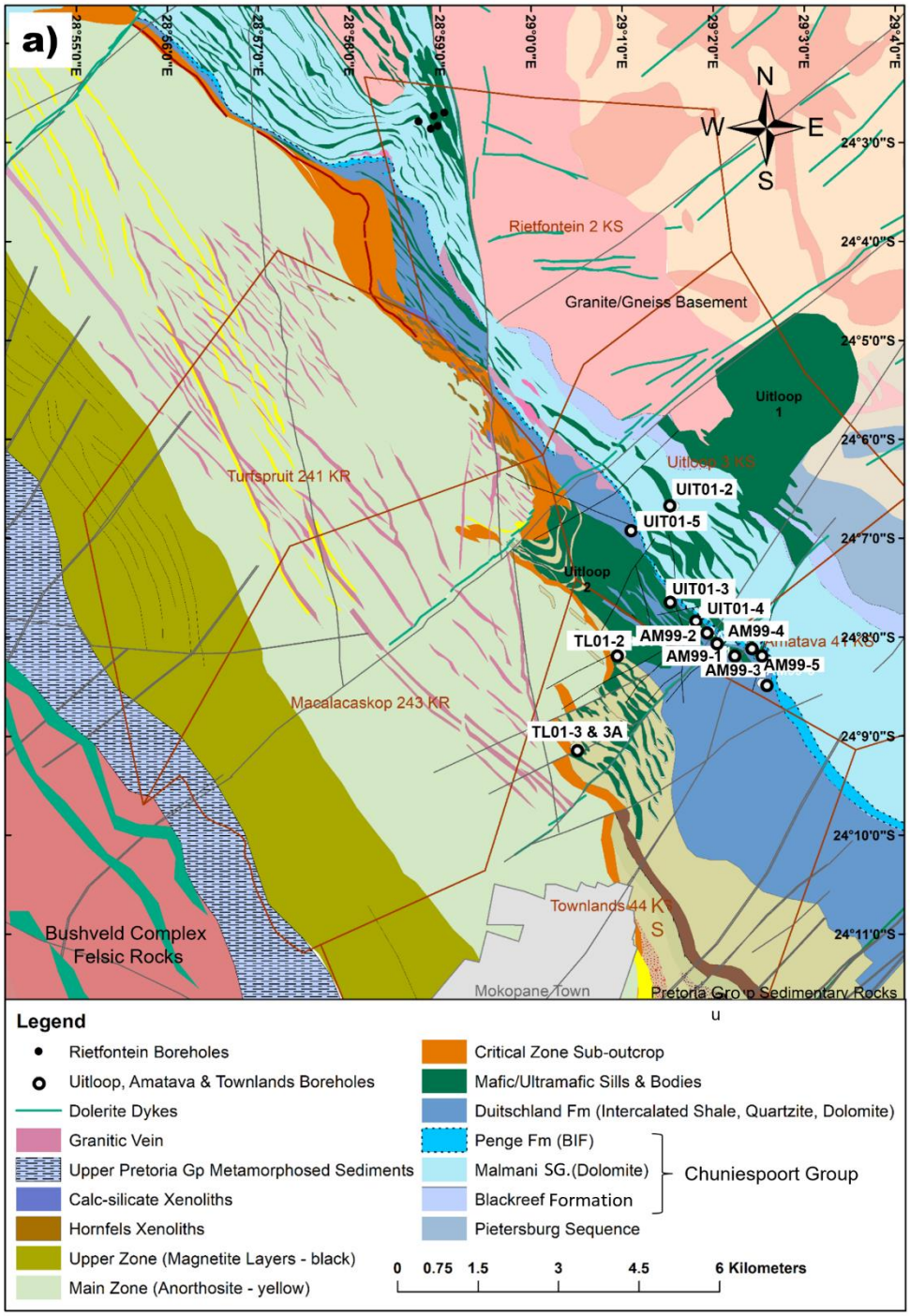
a)
28°55'0"E
28°56'0"E
28°57'0"E
28°58'0"E
28°59'0"E
29°0'0"E
29°1'0"E
29°2'0"E
29°3'0"E
29°4'0"E
N
W
E
S
24°3'0"S
24°4'0"S
24°5'0"S
24°6'0"S
24°7'0"S
24°8'0"S
24°9'0"S
24°10'0"S
24°11'0"S
Rietfontein 2 KS
Granite/Gneiss Basement
Uitloop 1
Uitloop 3 KS
Turfspruit 241 KR
UIT01-2
UIT01-5
Uitloop 2
UIT01-3
UIT01-4
AM99-2
AM99-4
TL01-2
AM99-1
AM99-3
AM99-5
Macalacaskop 243 KR
TL01-3 & 3A
Townlands 44 KS
Bushveld Complex Felsic Rocks
Mokopane Town
Pretoria Group Sedimentary Rocks
Legend
Rietfontein Boreholes
Uitloop, Amatava & Townlands Boreholes
Dolerite Dykes
Granitic Vein
Upper Pretoria Gp Metamorphosed Sediments
Calc-silicate Xenoliths
Hornfels Xenoliths
Upper Zone (Magnetite Layers - black)
Main Zone (Anorthosite - yellow)
Critical Zone Sub-outcrop
Mafic/Ultramafic Sills & Bodies
Duitschland Fm (Intercalated Shale, Quartzite, Dolomite)
Penge Fm (BIF)
Malmani SG.(Dolomite)
Blackreef Formation
Chuniespoort Group
Pietersburg Sequence
0 0.75 1.5 3 4.5 6 Kilometers

1052

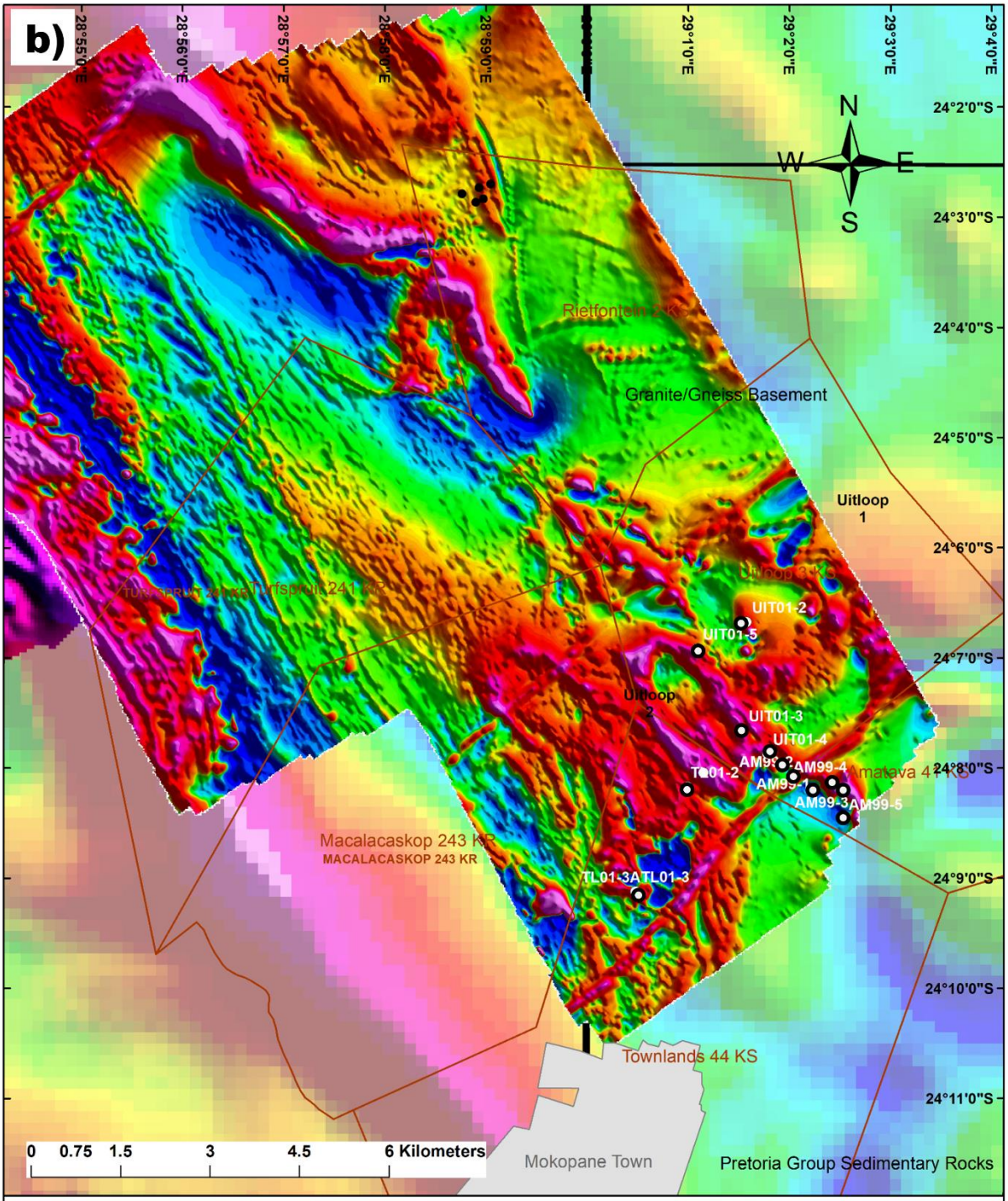

High resolution VRMI image (draped on regional TMI)

Rietfontein Boreholes

Uitloop, Amatava & Townlands Boreholes

Farm Boundaries

1053

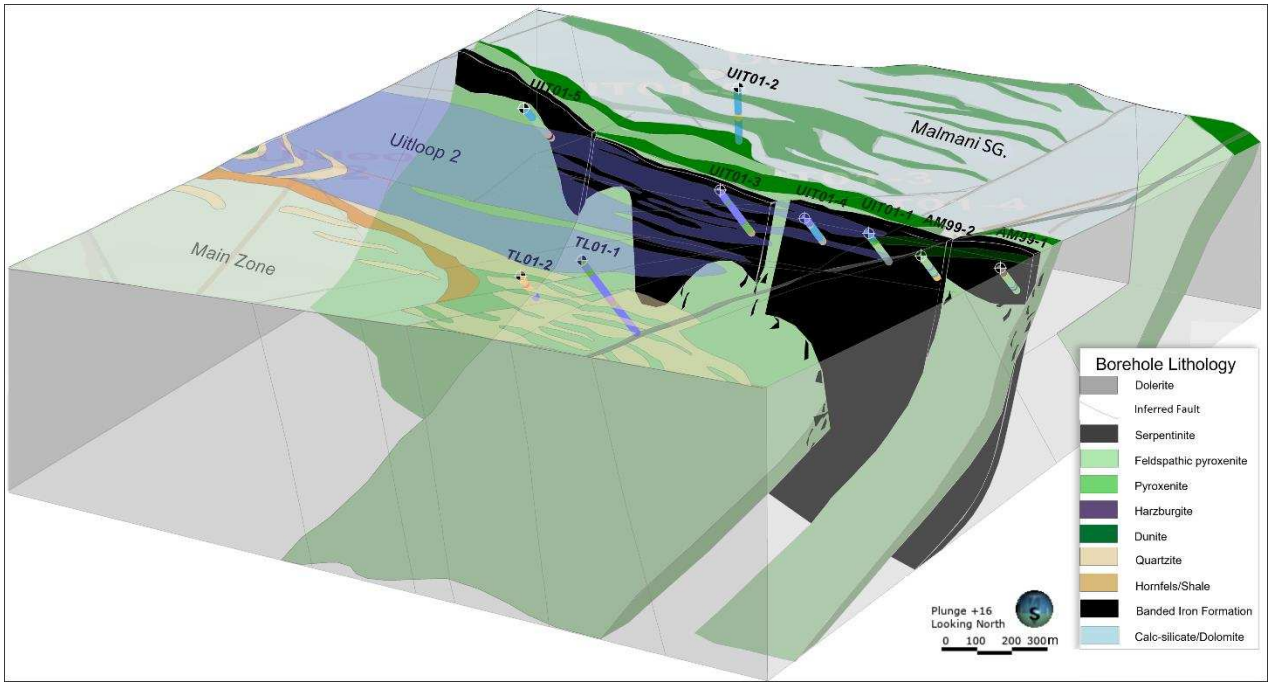
UIT01-2
Malmani SG.
Uitloop 2
Main Zone
TL01-2
TL01-1
AM99-2
Borehole Lithology
Dolerite
Inferred Fault
Serpentinite
Feldspathic pyroxenite
Pyroxenite
Harzburgite
Dunite
Quartzite
Hornfels/Shale
Banded Iron Formation
Calc-silicate/Dolomite
Plunge +16
Looking North
0 100 200 300m

1054

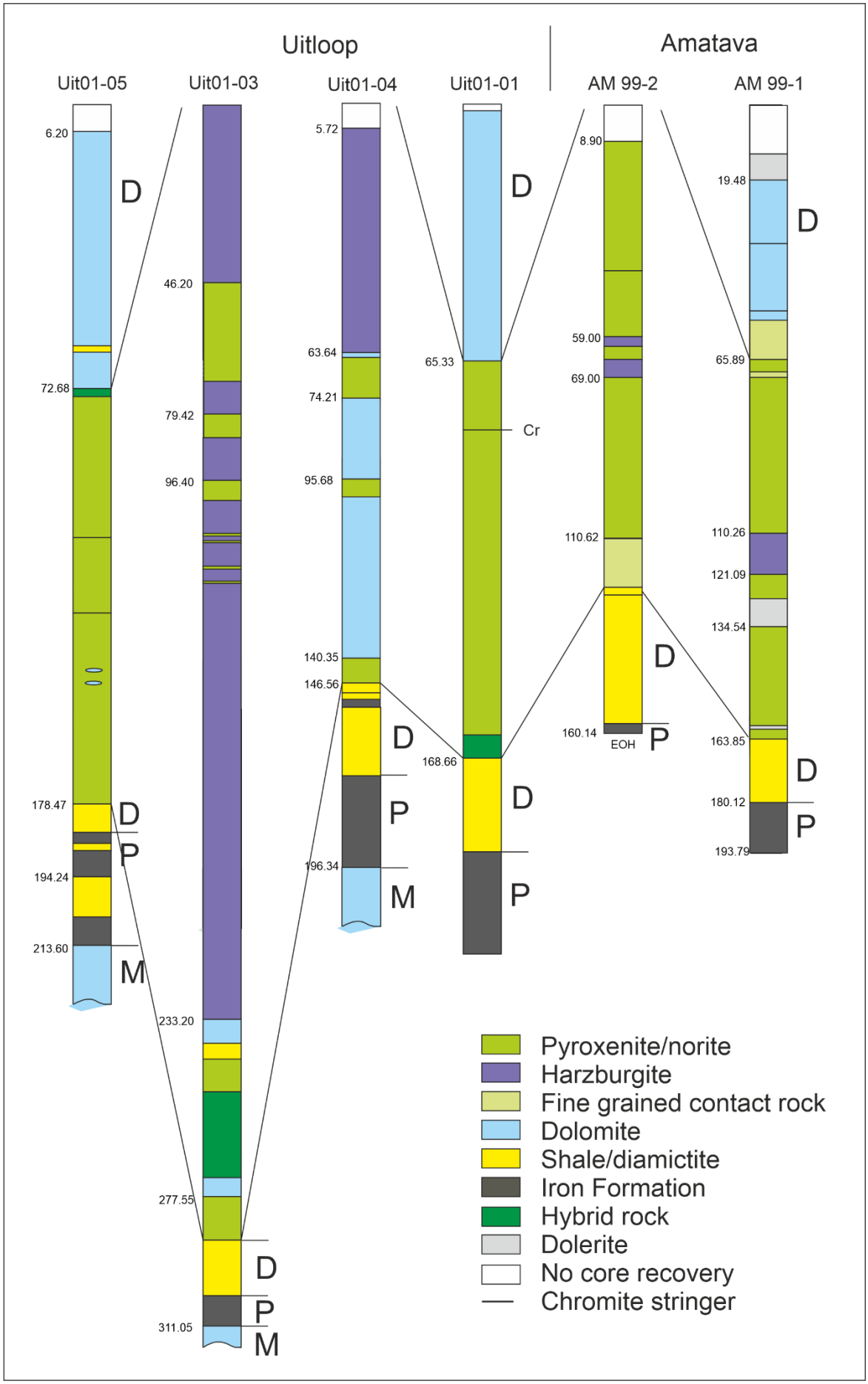
Uitloop
Amatava
Uit01-05
Uit01-03
Uit01-04
Uit01-01
AM 99-2
AM 99-1
6.20
72.68
178.47
194.24
213.60
46.20
79.42
96.40
233.20
277.55
311.05
5.72
63.64
74.21
95.68
140.35
146.56
196.34
65.33
168.66
8.90
59.00
69.00
110.62
160.14
EOH
19.48
65.89
110.26
121.09
134.54
163.85
180.12
193.79
D
P
M
Cr
Pyroxenite/norite
Harzburgite
Fine grained contact rock
Dolomite
Shale/diamictite
Iron Formation
Hybrid rock
Dolerite
No core recovery
Chromite stringer

1055

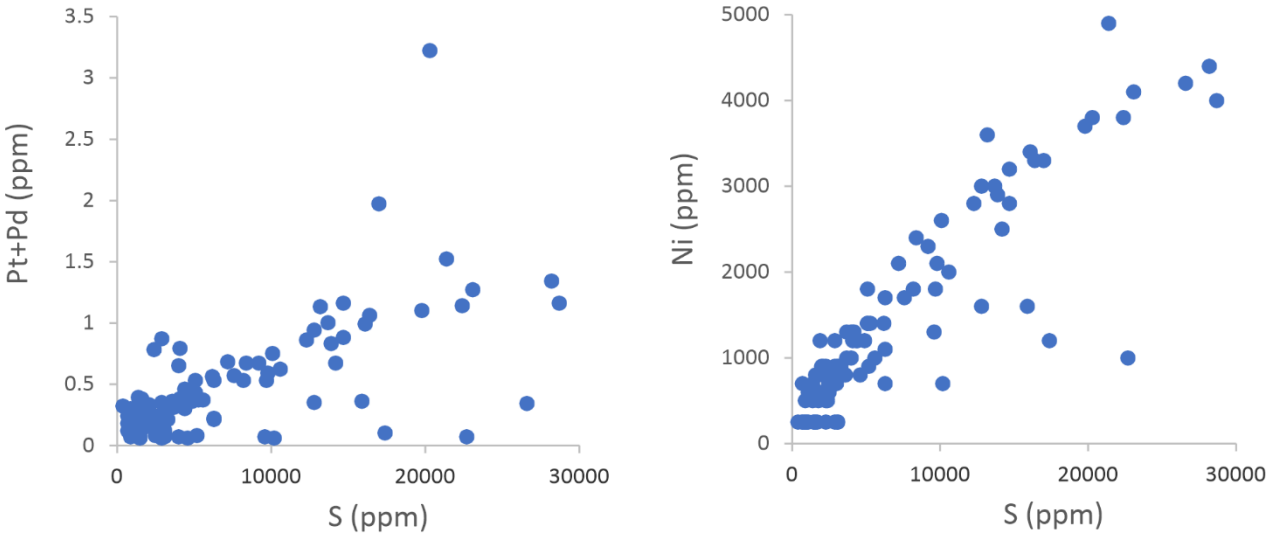
Pt+Pd (ppm)
S (ppm)
Ni (ppm)
S (ppm)

1056

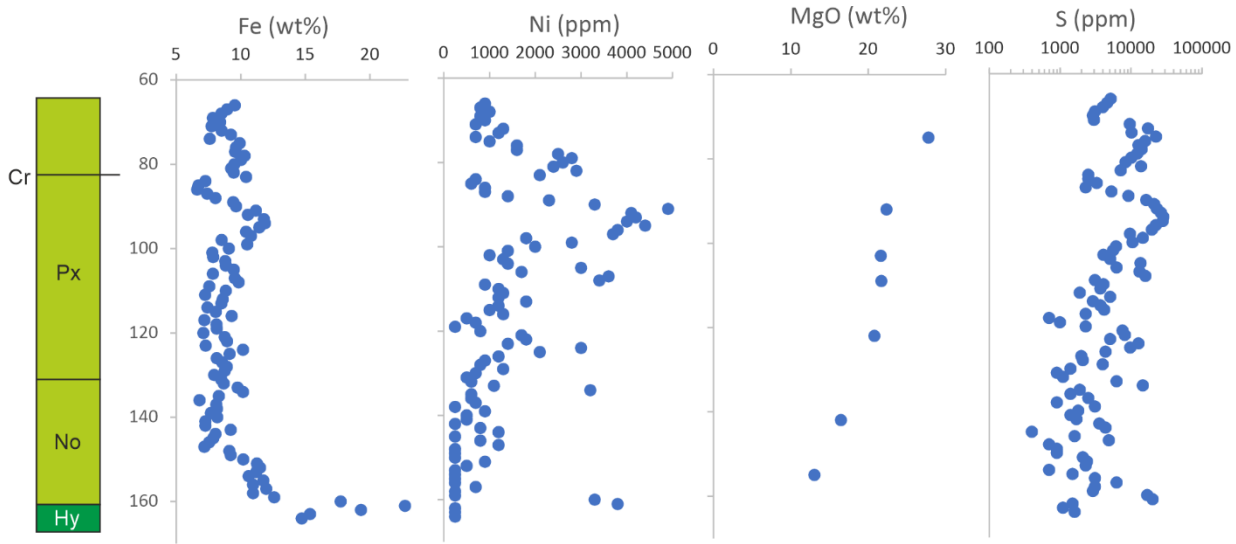
Fe (wt%)
Ni (ppm)
MgO (wt%)
S (ppm)
Cr
Px
No
Hy

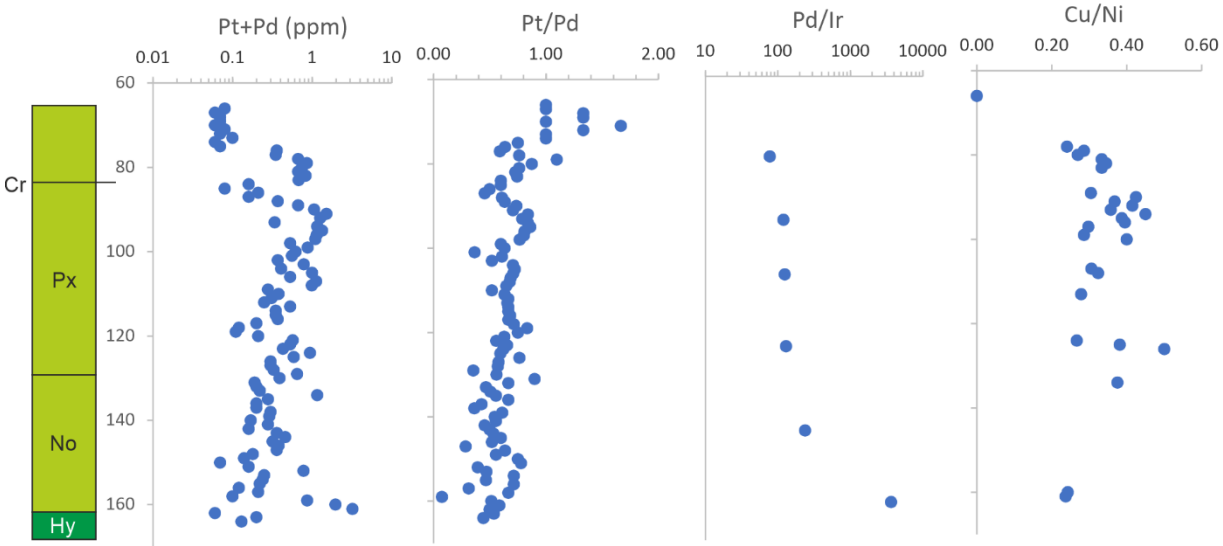
Pt+Pd (ppm)
Pt/Pd
Pd/Ir
Cu/Ni
Cr
Px
No
Hy

1057

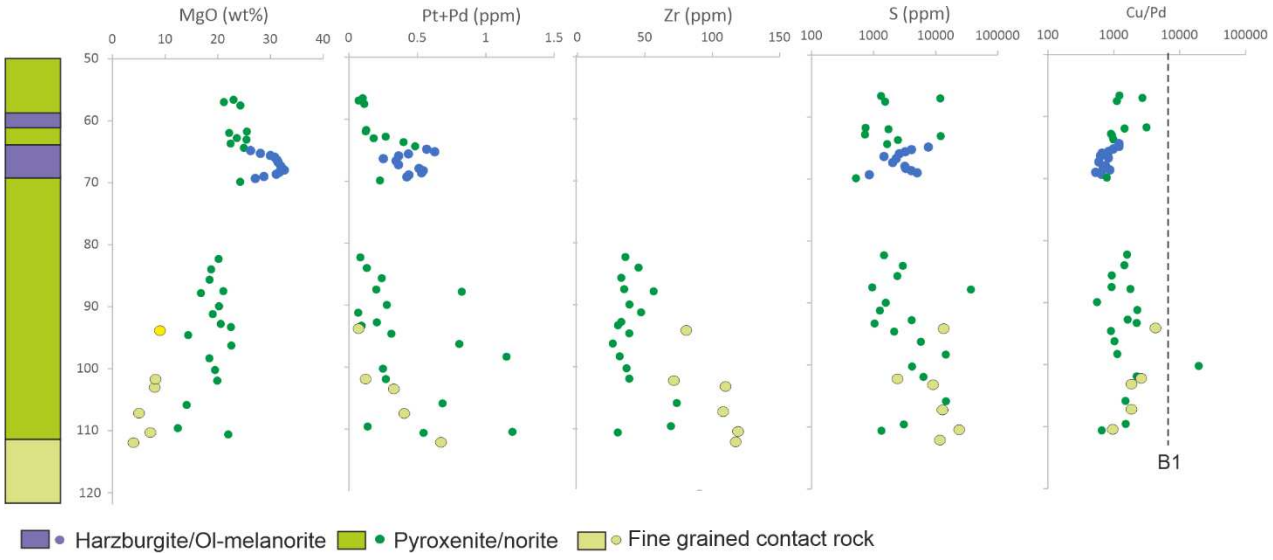
MgO (wt%)
Pt+Pd (ppm)
Zr (ppm)
S (ppm)
Cu/Pd
B1
Harzburgite/Ol-melanorite
Pyroxenite/norite
Fine grained contact rock

1058

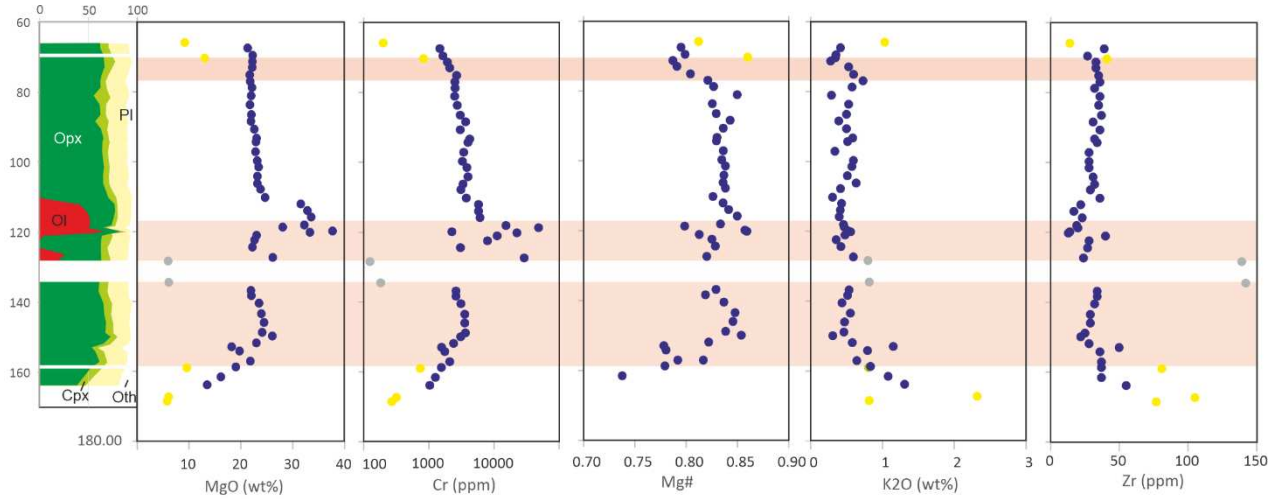
Opx
Pl
Ol
Cpx
MgO (wt%)
Cr (ppm)
Mg#
K2O (wt%)
Zr (ppm)

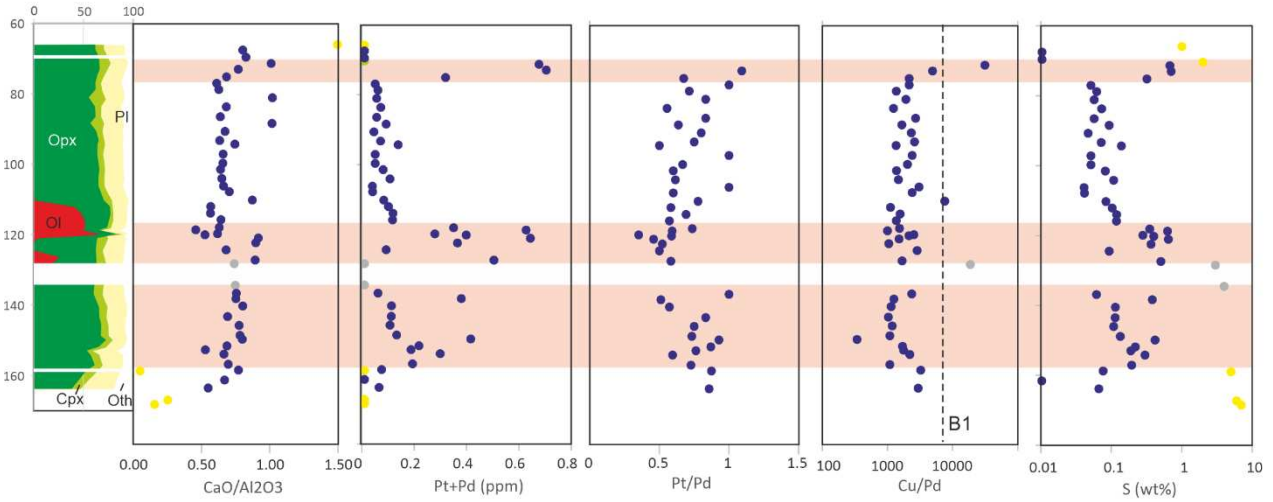
Opx
Pl
Ol
Cpx
CaO/Al2O3
Pt+Pd (ppm)
Pt/Pd
Cu/Pd
B1
S (wt%)
Fine grained contact rocks
Dolerite
Cumulate rocks

1059

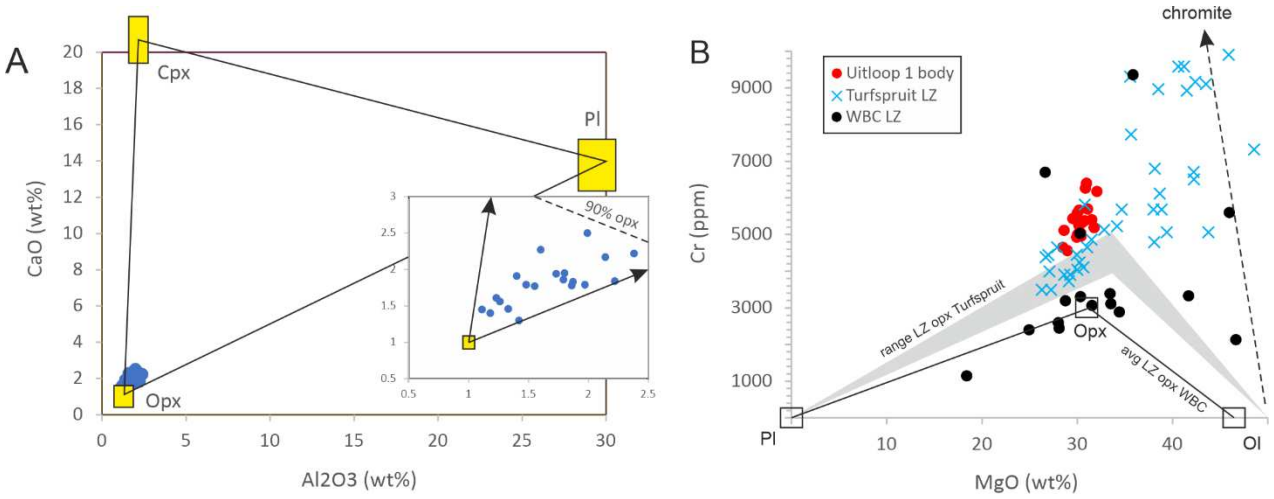
A
Cpx
Pl
Opx
90% opx
CaO (wt%)
Al2O3 (wt%)
B
chromite
Uitloop 1 body
Turfspruit LZ
WBC LZ
range LZ opx Turfspruit
avg LZ opx WBC
Opx
Pl
Ol
Cr (ppm)
MgO (wt%)

1060

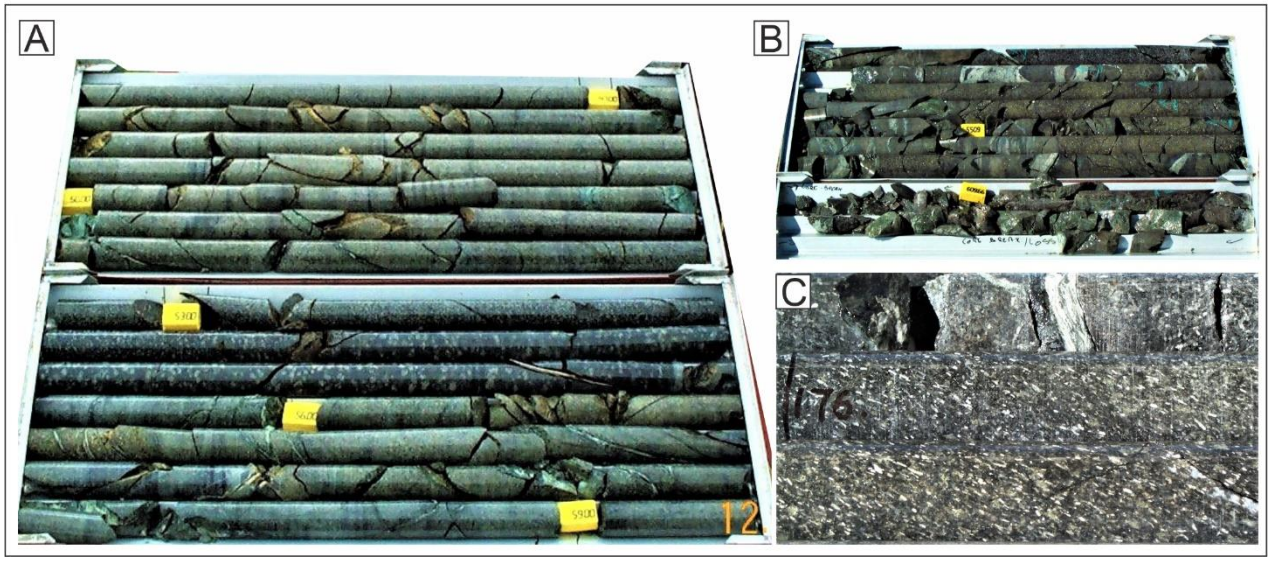
A
B
C

1061

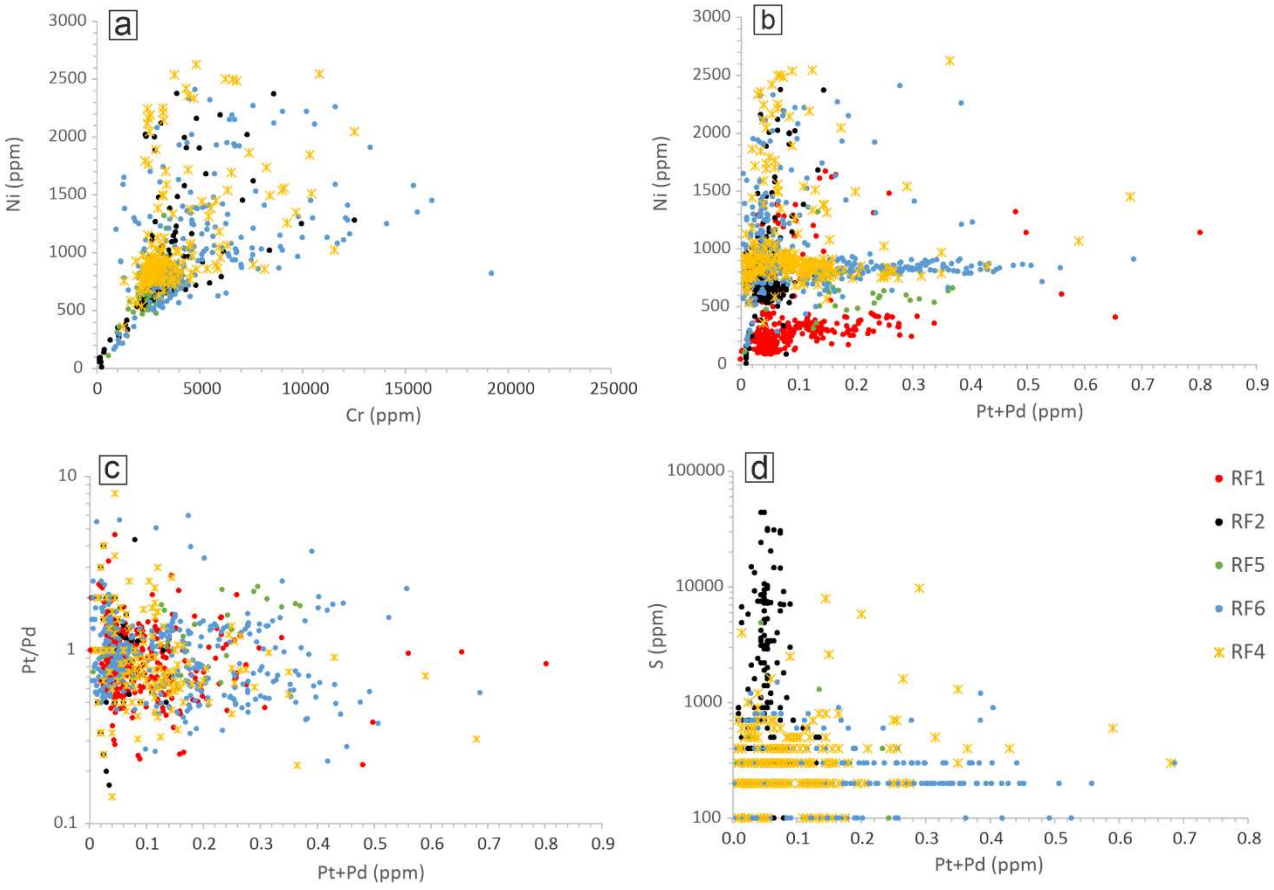

1062

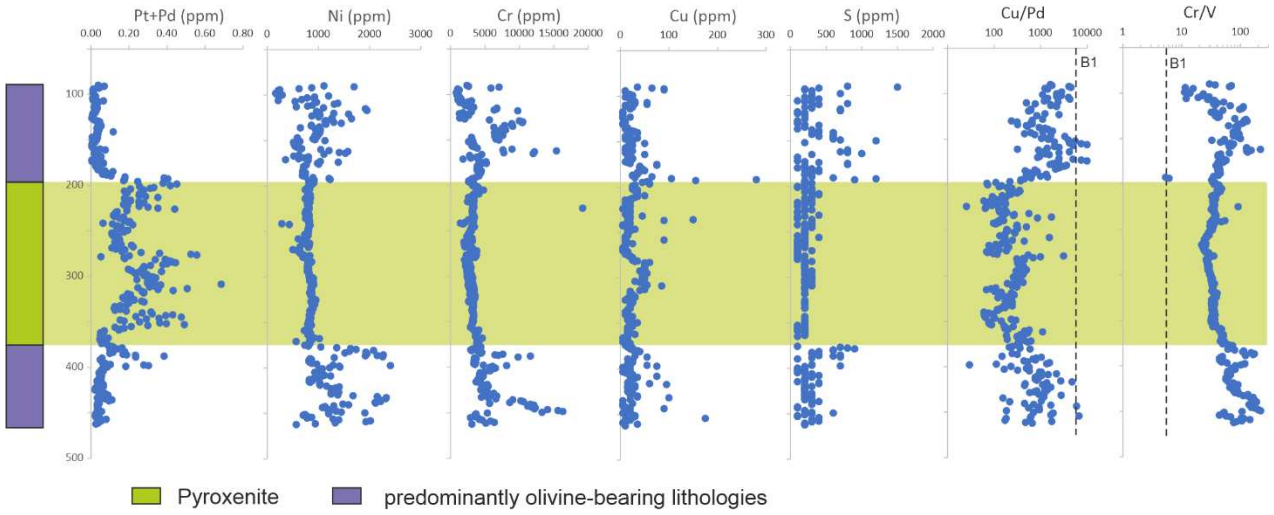

1063

Pyroxenite predominantly olivine-bearing lithologies

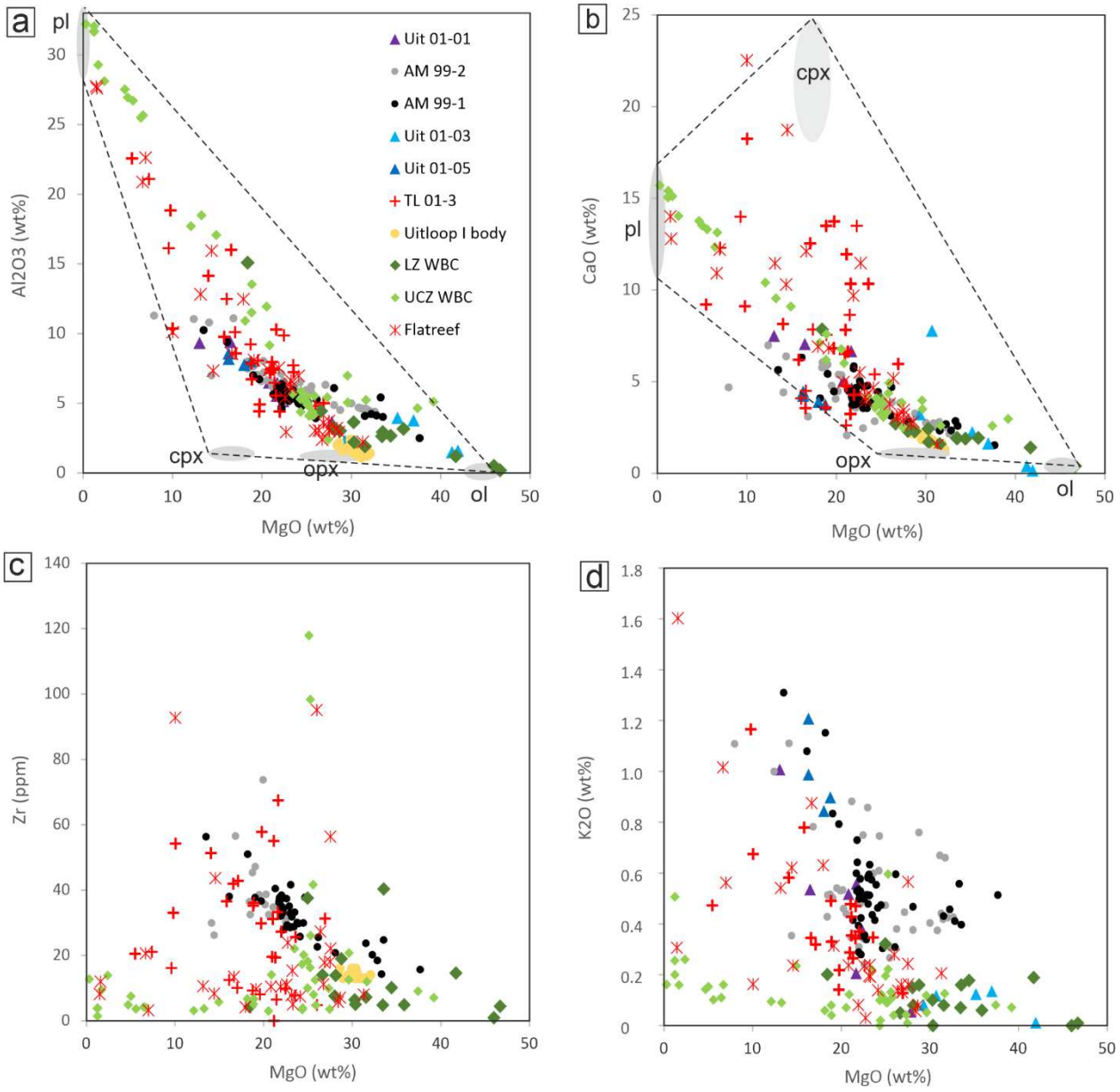
a
pl
cpx
opx
ol
Al2O3 (wt%)
MgO (wt%)
Uit 01-01
AM 99-2
AM 99-1
Uit 01-03
Uit 01-05
TL 01-3
Uitloop I body
LZ WBC
UCZ WBC
Flatreef
b
cpx
pl
opx
ol
CaO (wt%)
MgO (wt%)
c
Zr (ppm)
MgO (wt%)
d
K2O (wt%)
MgO (wt%)

1064

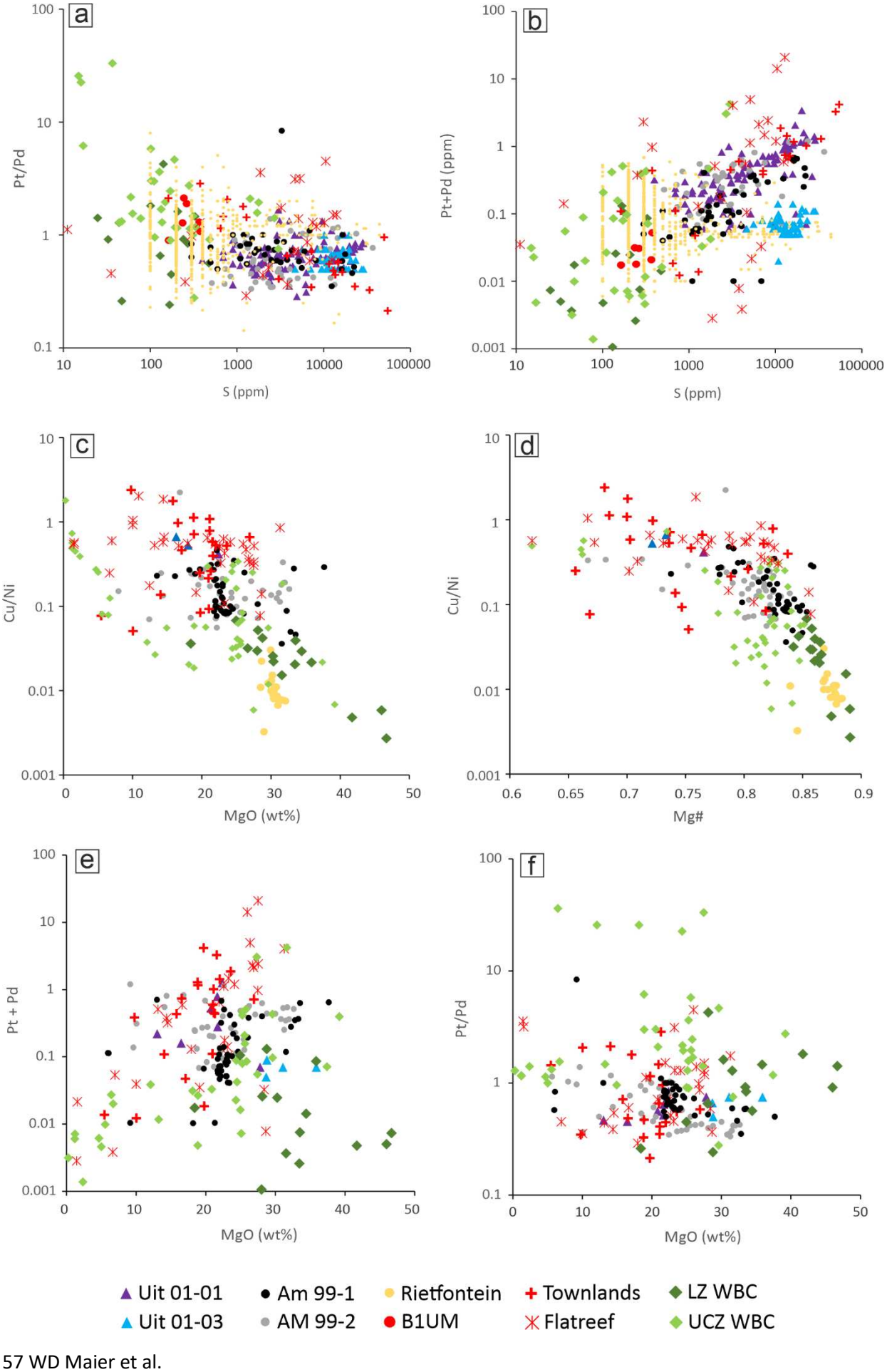
a
Pt/Pd
S (ppm)
b
Pt+Pd (ppm)
S (ppm)
c
Cu/Ni
MgO (wt%)
d
Cu/Ni
Mg#
e
Pt + Pd
MgO (wt%)
f
Pt/Pd
MgO (wt%)
Uit 01-01
Uit 01-03
Am 99-1
AM 99-2
Rietfontein
B1UM
Townlands
Flatreef
LZ WBC
UCZ WBC

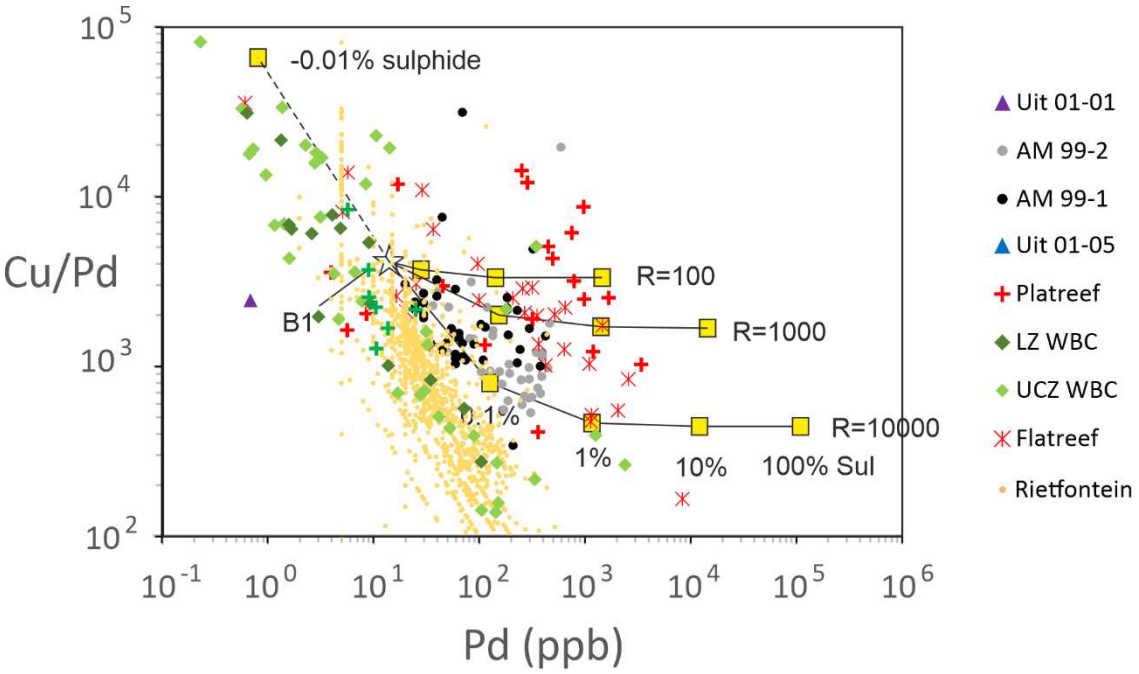
-0.01% sulphide
R=100
R=1000
R=10000
B1
0.1%
1%
10%
100% Sul
Cu/Pd
Pd (ppb)
Uit 01-01
AM 99-2
AM 99-1
Uit 01-05
Platreef
LZ WBC
UCZ WBC
Flatreef
Rietfontein

1066

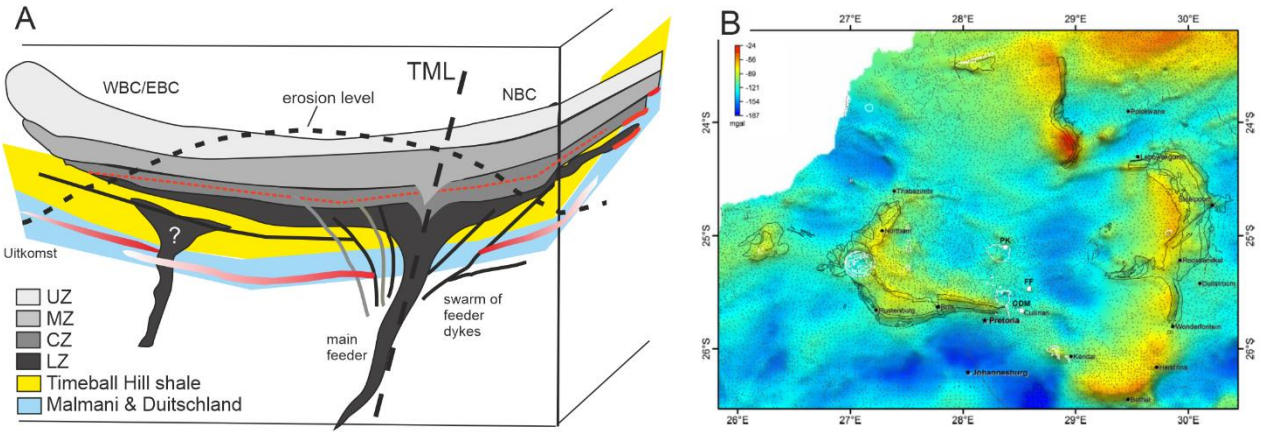
A
WBC/EBC
erosion level
TML
NBC
Uitkomst
?
UZ
MZ
CZ
LZ
Timeball Hill shale
Malmani & Duitschland
main feeder
swarm of feeder dykes
B

1067